A COMPARATIVE STUDY ON THE PHOTOCATALYTIC ACTIVITY OF DYE-SENSITIZED AND NON-SENSITIZED GRAPHENE OXIDE-TiO$_2$ COMPOSITES UNDER SIMULATED AND DIRECT SUN LIGHT

A Thesis Submitted to
Graduate School of Engineering and Sciences of
İzmir Institute of Technology
in Partial Fulfillment of the Requirements for the Degree of

MASTER OF SCIENCE

in Photonics Science and Engineering

by
Hatice İLHAN

December 2019
İZMİR

We approve the thesis of **Hatice İLHAN**

Examining Committee Members:

Prof. Dr. Canan VARLIKLI
Department of Photonics, İzmir Institute of Technology

Assoc. Prof. Dr. Sinan BALCI
Department of Photonics, İzmir Institute of Technology

Prof. Dr. Hülya AYAR KAYALI
Department of Chemistry, Dokuz Eylül University

16 December 2019

Prof. Dr. Canan VARLIKLI
Supervisor, Department of Photonics, İzmir Institute of Technology

Prof. Dr. Mustafa Muammer DEMİR
Co-Supervisor, Department of Material Sciences and Engineering, İzmir Institute of Technology

Prof. Dr. Canan VARLIKLI
Head of the Department of Photonics

Prof. Dr. Mehtap EANES
Dean of the Graduate School of Engineering and Sciences

ACKNOWLEDGMENTS

ABSTRACT

A COMPARATIVE STUDY ON THE PHOTOCATALYTIC ACTIVITY OF DYE-SENSITIZED AND NON-SENSITIZED GRAPHENE OXIDE- TiO$_2$ COMPOSITES UNDER SIMULATED AND DIRECT SUN LIGHT

Amine modified graphene oxide (mGO) and TiO$_2$ composite was synthesized by low temperature hydrothermal method. Characterization of the synthesized material was carried out by using X-ray diffraction, X-ray photoelectron spectroscopy, and BET analysis techniques. The films of mGO:TiO$_2$ and formerly synthesized TiO$_2$, N-TiO$_2$, GO-TiO$_2$ and GO:N-TiO$_2$ were fabricated by doctor blade method and employed as photocatalysts for the photodegradation of Rhodamine-B (RhB) dye under simulated (Xe lamb) and direct sun-light. P25 was also used as reference photocatalyst for all of the synthesized ones. Photodegradation of RhB was monitored by UV-Vis spectroscopy.

Among all the catalysts, GO:N-TiO$_2$, the composite of GO and N-doped TiO$_2$, presented the best photocatalytic activity and although the activity of mGO:TiO$_2$ was better than the activities of P25 and TiO$_2$, it presented lower degradation rate constant even than that of the N-TiO$_2$. It is proposed that increased abundance of C-C bonds and decreased number of oxygenated functional groups on mGO:TiO$_2$, in addition to the morphological difference between GO (sheet like) and mGO (dot like) has great influence on their photocatalytic activities. Among the GO containing photocatalysts including mGO:TiO$_2$, specific surface area (SSA) and number of RhB molecules per film volume were the lowest and particle size was the highest for mGO:TiO$_2$. Although the number of RhB molecules per film volume was higher in mGO:TiO$_2$ than that of the N-TiO$_2$, it is thought that approximately 2 folds higher SSA of N-TiO$_2$ allowed better photocatalytic performance.

Additionally, the films were sensitized with PTE dye to obtain effective catalysts in visible region and reusability of the films were also tested. Degradation rate constants of all fabricated films have increased under both of the irradiation media and no significant change in rate constants were detected after the reusability tests.

ÖZET

YAPAY VE DOĞRUDAN GÜNEŞ IŞIĞI ALTINDA BOYA İLE DUYARLAŞTIRILMIŞ VE DUYARLAŞTIRILMAMIŞ GRAFEN OKSİT-TİO$_2$ KOMPOZİTLERİNİN FOTOKATALİTİK AKTİVİTESİNİN KARŞILAŞTIRMALI BİR ÇALIŞMASI

Amin modifiye grafen oksit (mGO) ve TiO$_2$ kompoziti, düşük sıcaklık hidrotermal yöntemi ile sentezlendi. Sentezlenen malzemenin karakterizasyonu, X-ışını kırınımı, X-ışını fotoelektron spektroskopisi ve BET analiz teknikleri kullanılarak gerçekleştirildi. mGO: TiO$_2$ filmleri ve daha önce sentezlenen TiO$_2$, N-TiO$_2$, GO-TiO$_2$ ve GO: N-TiO$_2$ filmleri, bıçak sıyırma yöntemiyle üretildi ve simüle edilmiş (Xe lamba) ve doğrudan güneş ışığı altında, Rhodamine-B (RhB) boyasının fotodegradasyonu için fotokatalizör olarak kullanıldı. P25, sentetik fotokatalizörlerin tümü için referans olarak kullanılmıştır. RhB'nin fotodegradasyon süreci UV-Vis spektroskopisi ile izlenmiştir.

Tüm katalizörler arasında GO ve N katkılı TiO$_2$ kompoziti olan GO: N-TiO$_2$, en iyi fotokatalitik aktiviteyi sergilemiştir ve mGO: TiO$_2$'nin aktivitesi, P25 ve TiO$_2$'nin aktivitelerinden daha iyi olmasına rağmen, N-TiO$_2$'den dahi düşük bozunma hız sabiti sunmuştur. GO (tabaka benzeri) ve mGO (nokta benzeri) arasındaki morfolojik farklılığa ek olarak, mGO: TiO$_2$ üzerinde C-C bağlarının bolluğunun artması ve oksijen içeren fonksiyonel grupların sayısının azalması, fotokatalitik aktiviteleri üzerinde büyük etkisi olduğu önerilmiştir. mGO:TiO$_2$ dahil GO içeren fotokatalizörler arasında, spesifik yüzey alanı (SSA) ve birim film hacmi başına RhB molekül sayısı mGO: TiO$_2$ için en düşük ve partikül büyüklüğü en yüksektir. Birim film hacmi başına RhB molekül sayısı mGO: TiO$_2$'de, N-TiO$_2$'den daha yüksek olmasına rağmen, yaklaşık 2 kat daha yüksek N-TiO$_2$ SSA' sının daha iyi fotokatalitik performansa izin verdiği düşünülmektedir.

Ek olarak, görünür bölgede etkili katalizörler elde etmek için, filmler PTE boyası ile duyarlaştırıldı ve filmlerin tekrar kullanılabilirliği de test edildi. Üretilen tüm filmlerin bozunma hızı sabitleri her iki ışık ortamı altında da artmıştır ve yeniden kullanılabilirlik testlerinden sonra hız sabitlerinde önemli bir değişiklik saptanmamıştır.

To my dear family

TABLE OF CONTENTS

LIST OF FIGURES

LIST OF TABLES

LIST OF SYMBOLS and ABBREVIATIONS

nm…………………………………………………………………………Nanometer

λ……………………………………………………………………Wavelength

Ǻ……………………………………………………………………...Angstrom

π……………………………………………………………………………Pi

β………………………………………………………Width of maximum scattering peak

θ……………………………………………………………Peak point

°K……………………………………………………………………..Kelvin

°C ………………………………………………………………..…Centigrade

υ……………………………………………υ………………………..Frequency

ℏ……………………………………………………………Planck constant

E_g……………………………………………………………Band gap Energy

e^-………………………………………………………………Electron

h^+ …………………………………………………………..Hole

eV………………………………………………………...Electron Volt

MO…………………………………………………………..Methyl Orange

MB…………………………………………………………Methylene Blue

RhB…………………………………………………....Rhodamine B

UV……………………………………………………….Ultraviolet

CO_2……………………………………………………..Carbon dioxide

TiO_2…………………………………………………..Titanium dioxide

WO_3………………………………………………… Tungsten trioxide

$SrTiO_3$……………………………………………….Strontium titanate

Fe_2O_3……………………………………………….........Iron Oxide

ZnO……………………………………………………Zinc Oxide

ZnS………………………………………………..Zinc Sulfide

CN^-………………………………………………….........Cyanide

O_2^- ………………………………………………..Superoxide Anion Radical

Cu…………………………………………………….........Copper

Cr…………………………………………………….......Chromium

Nb……………………………………………………….........Niobium

Ru…………………………………………………..Ruthenium

LIST OF SYMBOLS and ABBREVIATIONS (cont.)

N…………………………………………………………………………....Nitrogen

B…………………………………………………………………….............Boron

F…………………………………………………………………………....Fluorine

Co…………………………………………………………………………..Cobalt

Mn…………………………………………………………………Manganese

V……………………………………………………………………..Vanadium

Ag…………………………………………………………………...........Silver

C…………………………………………………………………...............Carbon

P……………………………………………………………………...........Phosphorus

Ni………………………………………………………………….......Nickel

Mo………………………………………………………………Molybdenum

Fe…………………………………………………………………...........Iron

Pt…………………………………………………………………......Platinum

S…………………………………………………………………….........Sulfur

I…………………………………………………………………….........Iodine

GO……………………………………………………………Graphene Oxide

RGO……………………………………………………………...Reduced Graphene Oxide

GO-TiO_2………………………………………………….....Graphene Oxide-Titanium Oxide

CVD……………………………………………………………Chemical Vapor Deposition

H_2SO_4………………………………………………….....................Sulfuric Acid

$KMnO_4$……………………………………………………………Potassium Permanganate

NO_2…………………………………………………………………..Nitrogen Dioxide

ClO_2………………………………………………………………Chlorine Dioxide

HNO_3…………………………………………………………...........Nitric Acid

N_2O_3…………………………………………………………...Dinitrojen Trioksit

SiC…………………………………………………………………….Silicon Carbide

RuO_2………………………………………………………………Ruthenium(IV) oxide

In…………………………………………………………………………Indium

MgO………………………………………………………………..Magnesium Oxide

CaO………………………………………………………………Calcium Oxide

SrO………………………………………………………………Strontium Oxide

Bi………………………………………………………………............Bismuth

NH_4OH…………………………………………………...Ammonium Hydroxide

KBr…………………………………………………..Potassium Bromide

H_2O_2…………………………………………………..Hydrogen peroxide

TTIP………………………………………………Titanium Tetraisopropoxide

EtOH……………………………………………………………...Ethanol

H_3PO_4……………………………………………………Phosphoric Acid

D…………………………………………………………..Crystal Size

SSA……………………………………………………...Specific Surface Area

B.E……………………………………………………..Binding Energy

XRD…………………………………………………...X-Ray Diffraction

XPS………………………………………………X-ray photoelectron spectroscopy

BET…………………………………………Brunauer, Emmett and Teller Analysis

FTIR…………………………………...Fourier-transform Infrared Spectroscopy

CHAPTER 1

INTRODUCTION

1.1. Waste Water Purification

Reaching clean water sources or keeping the water sources clean are the problems of both developed and undeveloped countries. Industrial development and increasing population increases the importance of this problem and make it one the top ten problems of the world (Smalley 2005). Therefore, removing contaminants and unwanted components from waste water or reducing their concentrations to make water suitable for the end-use has become an important issue (Mattos et al. 2019).

Water pollution occurs when effluents are discharged into water bodies such rivers, lakes and oceans and will modify the water in a negative fashion. It is reported that textile dyes and other industrial dyestuffs constitute one of the largest groups of organic compounds that represent an increasing environmental danger for water sources. Hazardous chemicals in wastewaters are difficult to decay. Annual production of textile dyestuffs worldwide is around 700,000 tons, but 50% of these dyestuffs are reactive dyestuffs containing azo group ($-N = N-$)(Marcano et al. 2010; Taşli et al. 2019). The superior properties of these dyestuffs are their rapid applicability and bright colors but 10-50% of them cannot react with textile fibers during dyeing process and are hydrolyzed and released into the ecosystem (Mahmoodi et al. 2005). These dyes, which have complex aromatic structures, are toxic and carcinogenic molecules (Rauf, Meetani, and Hisaindee 2011). The release of these colored wastes to the environment creates serious health problems and show mutagenic effects for living organisms in seas, lakes and rivers. In addition, the dye molecules present in the waste water can react with other chemicals through oxidation or hydrolysis reactions to form dangerous by-products (Guillard et al. 2005).

Considering that the need for clean water is increasing and water resources are becoming exhausted in the world, the importance of water treatment becomes more evident. Today, biological, physical and chemical treatment methods have traditionally been used in the removal of organic pollutants in the waste water and these techniques

are still being developed. It is even more important that these treatment activities are carried out economically and effectively. According to the recent reports, heterogeneous photocatalysis method with its advantages compared to traditional methods, has emerged as a promising solution in solving environmental pollution problems (Szczepanik 2017; Ahmed and Haider 2018; Munjal et al. 2017; Dong et al. 2015) .

Dyes are colored compounds used to give color to a variety of substrates such as textiles, paper, leather and other materials. Dyes which have affinity for effective application on fibers may attach by physically attractions (Van der Waals or ionic) or chemical (hydrogen bonds and/or covalent) bonds on the fibers. The structure of the dye comprises a chromophore which is responsible for its color and auxochrome groups that change the color of the dye (Hunger 2017). There are many ways to classify dyes, one of which is according to their use in the textile industry such as anionic, cationic and nonionic (Drahansky et al. 2016). It is also possible to divide them into subgroups as shown in Figure 1. 1.
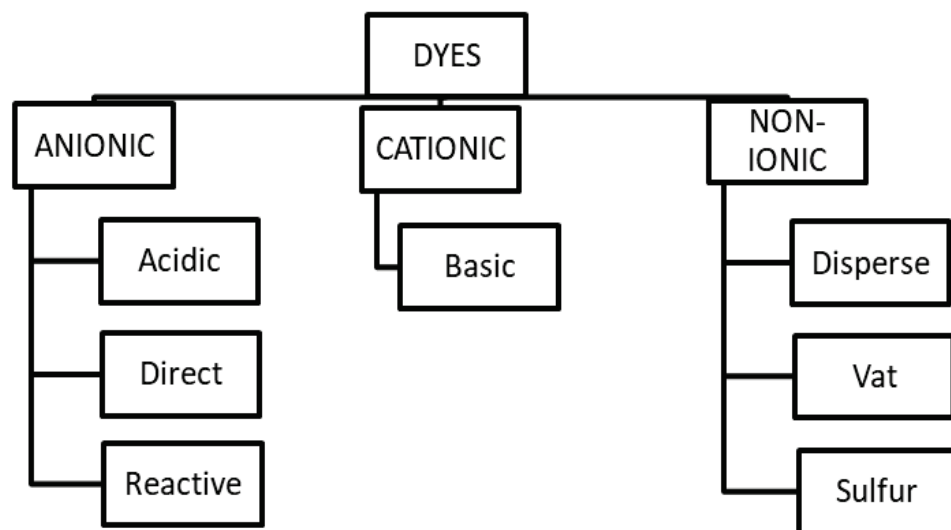
Figure 1. 1. Classification of dyes based on use in the textile industry.

Many dyes, including acidic, direct, mordant and reactive dyes, belong to anionic dye classes. Anionic dyes contain functional groups which are sodium salts of sulfonic or carboxylic acids. The dyes differ in the sub-classification of their affinity to the fibers and the presence of specific functional groups (Reynel-Avila, Mendoza-Castillo, and Bonilla-Petriciolet 2016).

The cationic dyes, which form the basic dye class, are highly bright and dense in color. Cationic dyes dissolve in water. They are used with acrylic, wool, nylon and silk fibers. This class of dye contains aromatic groups with different chemical structures and those aromatic groups can cause allergic reactions, serious skin irritations and even cancer. The cationic dye class includes cationic azo dyes and methane dyes, phthalasionine and polycarboxylic dyes. Examples of dyes of this class are methylene blue (MB), basic blue 41, crystal violet and basic red 46. MB is the most widely used dye among basic dyes, especially in textile. Another commonly used dye is the Rhodamine B (RhB). It is a red, basic dye used in textile and food industry fields and it is also most of the times used to simulate organic pollutants in photocatalytic studies (Adebowale, Olu-Owolabi, and Chigbundu 2014).

Biological treatment methods, physical separation methods (adsorption, sedimentation, ion exchange, etc.) and chemical treatment methods (chlorination, ozonation) are traditionally used for the removal of organic pollutants in waste water.

Biological treatment is generally cheaper than physical and chemical methods. Biodegradation of a chemical is the removal of pollution by the metabolic activities of living organisms. It is generally carried out by microorganisms, especially bacteria and fungi. However, as many toxic mixtures are lethal to microorganisms as well, some chemicals cannot be biodegraded. Therefore, the use of biological removal methods alone is limited.

Adsorption and membrane filtration are some of the physical methods applied. The disadvantage of these methods is that organic pollutants can only be removed from water, and that organic pollutants are not completely decomposed. In any case, these techniques earn their reputation and therefore short descriptions are provided in this thesis: *Adsorption* is an economical and efficient technique for removing stable contaminants. There are two mechanisms in color removal; adsorption and ion exchange. The effectiveness of this method is influenced by factors such as the interaction of the dye with the adsorbent material, surface area of the adsorbent, particle size, temperature and pH. The most commonly used adsorbent is activated carbon. It is especially effective on cationic, mordant and acidic dyes. The effectiveness of activated carbon depends on the characteristics of the wastewater and the type of carbon. The removal rate strongly depends on the amount of carbon used and therefore the cost of activated carbon limits the use of the method (Ali 2012). *Membrane filtration* method contains membranes which form a barrier for some substances and allow others to pass

through. Their superiority over other methods is defined as being resistant to temperature, changing chemical environment and microbial attacks. However, the removal of residual waste after separation from water and the replacement of the membrane with a new one will result in increased operating costs (Robinson et al. 2001).

Chemical methods include oxidative methods (hydrogen peroxide-fenton reagent) and ozonation methods. In some of the chemical methods coagulants are also used to assemble the particles and increase the particle size (Purkait et al. 2004). Oxidizing agents (e.g. H_2O_2) in the presence of UV light is used in *Oxidative method*. In this method, the aromatic ring of the dye molecule is broken and the dyes in the waste water are removed (Slokar and Majcen Le Marechal 1998). The separation process may also be carried out by activating H_2O_2 with iron salts (fenton reagent). The Fenton reagent *(H_2O_2-Fe (II))* is suitable for species resistant to biological treatment in wastewater. However, application of this method results in secondary pollutants generating from the agents and dye molecules (Slokar and Majcen Le Marechal 1998). Ozone, is a better agent than other oxidation agents (chlorine, H_2O_2), is used in *ozonation*. It results in colorless small molecules as ozone breaks conjugated double bonds. However, these small molecules can increase the carcinogenic properties of waste water and in order to overcome this problem a second treatment is required which needs the continuation of the process and thus increases the operating costs (Robinson et al. 2001).

In summary, the described methods have bottlenecks in dose adjustment, toxic product formation, high cost and secondary pollution. For these reasons, semiconductor based photocatalytic studies have attracted attention in recent years. In this method, the catalyst materials are activated with the help of UV or visible light and organic compounds are decomposed to CO_2 and H_2O (Hudaya 2008). The photocatalytic degradation method involves both physical and chemical processes.
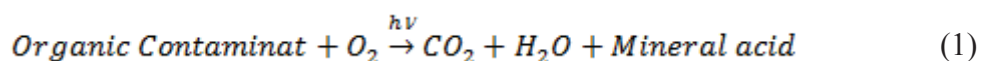
1.2. Photocatalytic Process

The photocatalytic degradation process is the degradation of organic- inorganic substances as a result of chemical reactions of the system consisting of natural sunlight

or UV light source and photocatalyst. The process includes a photon energy source to remove unwanted contaminants and have proven to be an effective and inexpensive way of removing organic and inorganic pollutants from water (Van Gerven et al. 2007). The degradation of pollutants in water by using sunlight has advantages such as considerably low energy requirements and on-site treatment compared to other treatment technologies (Parent et al. 1996). In the studies, it is also stated that the degradation of pollutants by sunlight in the presence of catalyst in natural environment is not only effective in countries with abundant sun but in all areas those can benefit more or less from the sun. Most importantly, this technology has many similarities with nature's self-cleaning mechanism. It can be easily applied to UV water treatment systems and can efficiently be used in a real environment (Sobczyński and Dobosz 2001).

Photocatalysis is the activity occurring when a light source interacts with the surface of semiconductor materials, the so called photocatalysts. During this process, at least two simultaneous reactions occur; oxidation from photogenerated holes, and reduction from photogenerated electrons. Photocatalysis creates strong oxidation agents to decompose any organic compound to CO_2 and HO_2 in the presence of photocatalyst and light (Gaya and Abdullah 2008). There are many parameters that are effective in photocatalytic degradation processes; surface area, particle size, surface hydroxyl groups and amount of *photocatalyst*, initial amount of *organic matter*, temperature and pH of the *media* and *light source* (Diker et al. 2011; Hudaya 2008).

1.2.1. Photocatalyst and Titanium dioxide (TiO_2) in photocatalysis

The photocatalyst is a semiconductor in which strong oxidation occurs on the surface by means of energy of light. The main function of photocatalyst is to increase the rate of reaction by reducing the activation energy. The overall equation of contaminant degradation in the presence of a semiconductor photocatalyst is given in Equation (1) (Gaya and Abdullah 2008) and the process is schematized in Figure 1.2.

$$Organic\ Contaminat + O_2 \xrightarrow{h\nu} CO_2 + H_2O + Mineral\ acid \qquad (1)$$
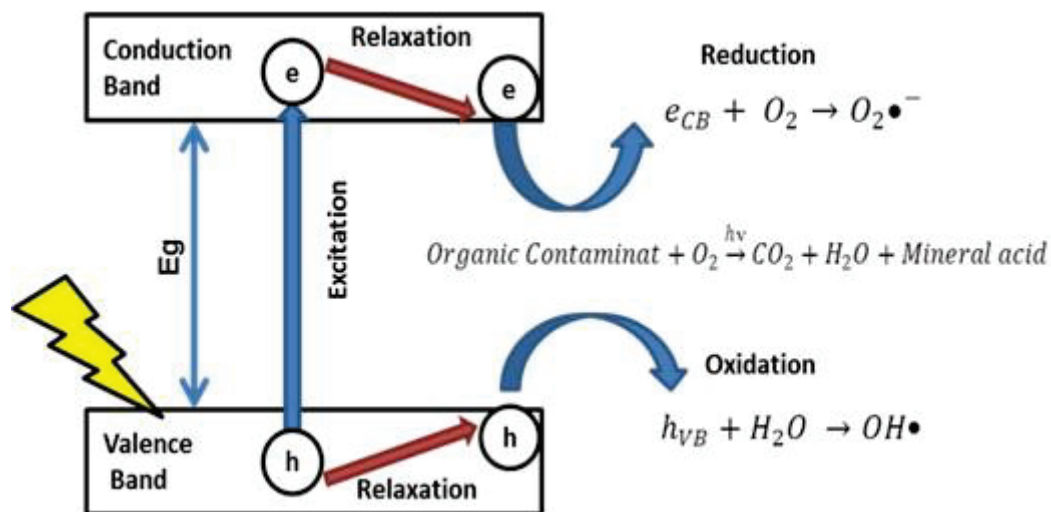
Figure 1. 2. Photocatalytic degradation mechanism

When the semiconductor is illuminated by a light source with higher energy than its band gap energy (E_g), the electrons in the valence band are excited to the conduction band leaving a hole behind. The formation of these electron-hole pairs (e^- - h^+) is the beginning of the photocatalysis process. The electron-hole pairs migrate to the particle surface in aqueous media and initiate various chemical reactions. The photogenerated holes are very strong oxidants and can oxidize many organic materials directly or react with water molecules on the surface of the photocatalyst to form highly reactive hydroxyl radical ($OH\bullet$). Generated electrons form superoxide anion radical ($O_2\bullet^-$) by reducing the adsorbed O_2 on the particle surface. This superoxide anion radical then reacts with water to form the $OH\bullet$ radical and increases the hydroxyl radical concentration in the medium. Both holes and hydroxyl radicals are very strong oxidants and can be used to oxidize organic materials (Nosaka and Nosaka 2016). $OH\bullet$ radicals are highly active and non-selective electrophilic particles; they attack organic molecules and decompose them down into small molecules such as H_2O, CO_2 and mineral acids. The formation processes of the reactive radicals are summarized below by using TiO_2 as photocatalyst [Equation (2)-(4)]. Perhydroxyl radical $HO_2\bullet$ is formed with reaction of $O_2\bullet^-$ and H^+ ions under acidic conditions. The perhydroxyl radical then forms hydrogen peroxide [Equation (5)-(7)]. The resulting H_2O_2, breaks down to form an $OH\bullet$ radical. Additionally, H_2O_2 acts as an electron acceptor, preventing the recombination of the pairs [Equation (8)-(10)]. In the absence of suitable acceptor states on or around the excited semiconductor, the resulting electron-hole pairs are recombined (Equation

11). This recombination occurs between energy bands or on the surface and reduces the efficiency of the process (Gaya and Abdullah 2008).

$$TiO_2 \xrightarrow{h\nu} h_{VB} + e_{CB} \tag{2}$$

$$h_{VB} + H_2O \rightarrow OH\bullet \tag{3}$$

$$e_{CB} + O_2 \rightarrow O_2\bullet^- \tag{4}$$

$$O_2\bullet^- + H^+ \rightarrow HO_2\bullet \tag{5}$$

$$O_2\bullet^- + HO_2\bullet \rightarrow HO_2^- + O_2 \tag{6}$$

$$HO_2^- + H^+ \rightarrow H_2O_2 \tag{7}$$

$$H_2O_2 \xrightarrow{h\nu} 2OH\bullet \tag{8}$$

$$H_2O_2 + e_{CB} \rightarrow OH\bullet + OH^- \tag{9}$$

$$H_2O_2 + O_2\bullet^- \rightarrow OH\bullet + OH^- + O_2 \tag{10}$$

$$h_{VB} + e_{CB} \rightarrow heat \tag{11}$$

TiO_2 is the most widely used metal oxide semiconductor in photocatalytic degradation process. As stated above, the band gap energy which is specific each semiconductor, plays an important role in the efficiency of the photocatalyst. The band gap energies of some semiconductors are given in Figure 1. *3* together with their valance and conduction band energy levels. The ability of the semiconductor-based material to degrade organic pollutants depends on the band energy potential of the semiconductor and the reduction / oxidation potential of the adsorbed particle. In order for the adsorbed particle to be reduced and to form superoxide anion radical $(O_2\bullet^-)$, the conductivity band potential of the semiconductor must be more negative than the reduction potential of the adsorbed particle. And in order for the adsorbed particle to be oxidized and to form the hydroxyl radical, the valence band potential of the semiconductor must be more positive than the oxidation potential of the adsorbed

particle. The band gap energy diagram of some semiconductors is shown in Figure 1. 3 (Hudaya 2008; Fujishima, Zhang, and Tryk 2008; Varlikli and Diker in Aliofkhazraei 2014).
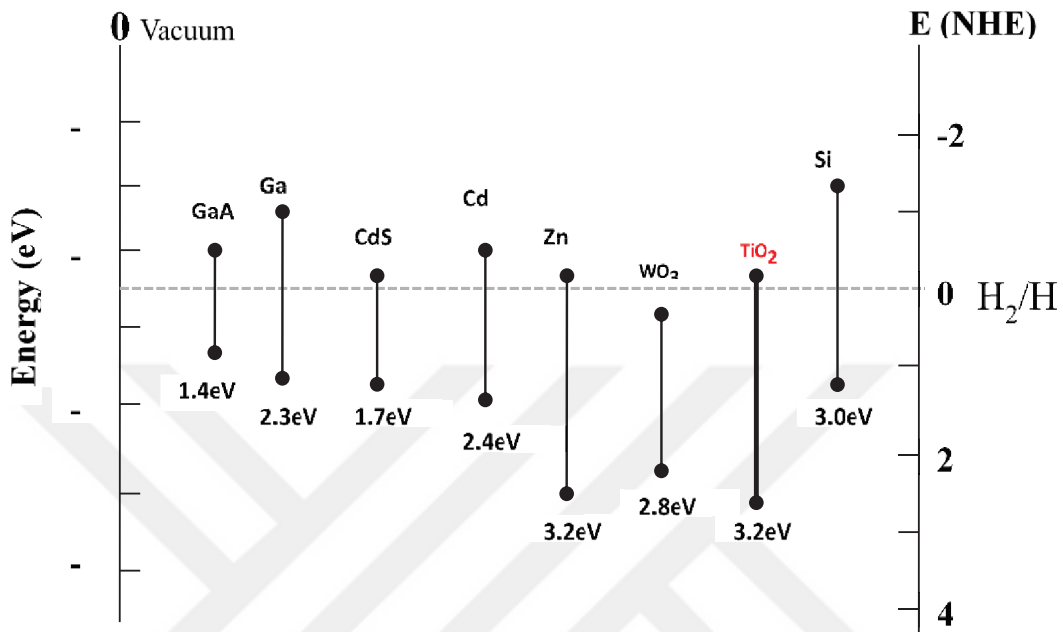
Figure 1. 3. Band gap energy diagrams of some semiconductors.

Although some semiconductors have sufficient band gap energy to catalyze or initiate reactions, they cannot be used as photocatalysts for various reasons. For example: the band gap energy of ZrO_2 is quite large (5eV) and therefore requires UV region excitation (Gaya and Abdullah 2008; Hudaya 2008), although the band gap energy of CdS is 2.5 eV the life time of photogenerated electron is quite short and ZnO is unstable in aqueous media. TiO_2, WO_3, $SrTiO_3$, Fe_2O_3, ZnO and ZnS are some of the well-studied semiconductor photocatalyst materials (Y. Li et al. 2019). Among them, TiO_2 is preferred because of its high productivity, low toxicity, excellent physical and chemical stability, and low cost.

TiO_2 has many applications due to its optical, electrical and chemical properties such as, water treatment, self-cleaning materials, sterilization processes, lithography processes, degradation of organic compounds and corrosion prevention of metal (Varlikli and Diker in Aliofkhazraei 2014). Titania powders are known and used since ancient times because of its harmless, low cost, chemical stability and due to its strong

white color it is used as a pigment material in toothpaste and sun creams. Among the metal-oxide semiconductors, TiO$_2$ is the most popular and widely used material for photocatalysts in the removal of resistant organic pollutants in water (Y. Li et al. 2019).

At the beginning of the 20th century, a lot of research has been done in the field of its photoactivity. Fujima and Honda achieved electrochemical photocatalysis of water at a semiconductor electrode in 1972 (Fujima, A., Honda 1972). Frank and Bard first reported the application of TiO$_2$ in the photocatalytic oxidation of CN^- and SO_3^{2-} in an aqueous system under sunlight (Frank and Bard 1977). Later, TiO$_2$ has been studied with great interest by many researchers as photocatalysts. The characteristic features of TiO$_2$ are, strong oxidation ability, high chemical and photochemical stability, long durability, non-toxic, corrosion resistant, low cost, insoluble and superhydrophilic behavior for organic pollutants.

TiO$_2$ crystallizes in three different phases: anatase, rutile and brokite. While rutile is a stable phase in tetragonal structure, anatase and brokite are crystallized in semi-stable structure and anatase tetragonal, brokite orthorhombic phase. Brokite phase does not have photocatalytic property. Although the anatase phase has higher band energy than rutile, it exhibits higher photocatalytic activity than rutile in many reactions. It is discussed in the literature in a way that the surfaces of the particles which have rutile form absorb less oxygen and this leads to the recombination of electron-hole pairs (Varlikli and Diker in Aliofkhazraei 2014). The presence of a low number of hydroxyl groups on the surface of the rutile leads to a low amount of reactant material adsorption. Adsorption of toxic molecules onto the catalyst surface is one of the important parameters in photocatalytic activity. The degradation process begins with adsorption of organic molecules on the photocatalyst surface.

In most of the photocatalysis systems, TiO$_2$ is added to the polluted medium in particle form and suspensions are obtained. The disadvantage of using the photocatalyst in suspension is the difficulty in separating it from the reaction medium; additional processes and extra costs are required to remove the catalyst. There are a few studies in the literature on the degradation of organic dyes using TiO$_2$ photocatalyst in thin film phase and they have exhibited lower photocatalytic activity due to the smaller contact area compared to that of the suspension phase (D. Wang et al. 2012; Ersundu 2017). However, the film phase is more suitable for reusability and applicability to a wide range of industrial wastes.
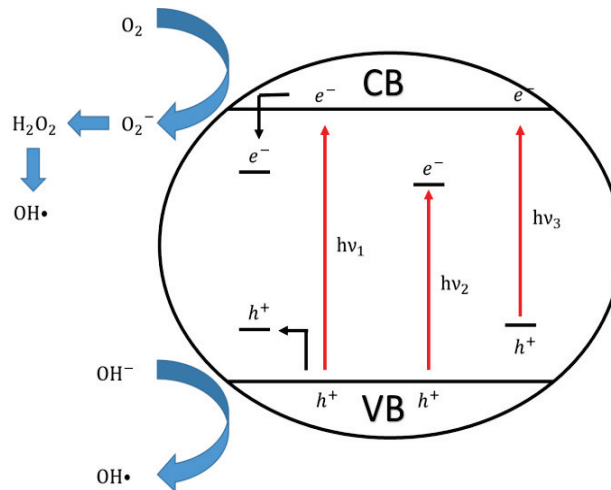
Figure 1.4. Photocatalytic degradation mechanism of TiO$_2$ by different doping methods; hv1: pure TiO$_2$, hv2; metal-doped and hv3; non-metal ion doped.

1.2.2 Photocatalyst and Graphene Derivatives in Photocatalysis

Graphene and graphene derivatives have received great interest due to their superior properties that leads to revolutionary advances in technology. The great interest of graphene and its derivatives started in 2004 with the first synthesis of graphene by Novolesov and Geim. They were able to isolate graphene as a monolayer from graphite, an allotrope of the carbon element. Using a Scotch tape, the graphite layer was peeled off the pencil and transferred to the SiO$_2$ substrate stably (Novoselov et al. 2004). Geim and Novoselov were awarded the Nobel Prize in Physics in 2010 for pioneering research on the structure and properties of graphene. The development of graphene has continued with the discovery of features that allow it to break many records for various application fields (Patel and Kiani 2019).

Graphite is the most stable of all commonly known allotropes of carbon. In graphite, carbon atoms are in the form of layers stacked on top of each other and the distance between layers is 0.335 nm. Within each layer of graphite, carbon atoms form strong covalent bounds to join one another with a molecular length 0.142 nm. However, there is no covalent bond between the layers; they are held together by Van der Walls interactions that make graphite soft and slippery. Graphene sheets can be exfoliated from graphite and this is possible due to weak forces between the graphite sheets when compared to strong covalent forces in the graphite sheets (Terrones et al. 2010). Figure 1. 5 shows the structure of graphite and graphene.
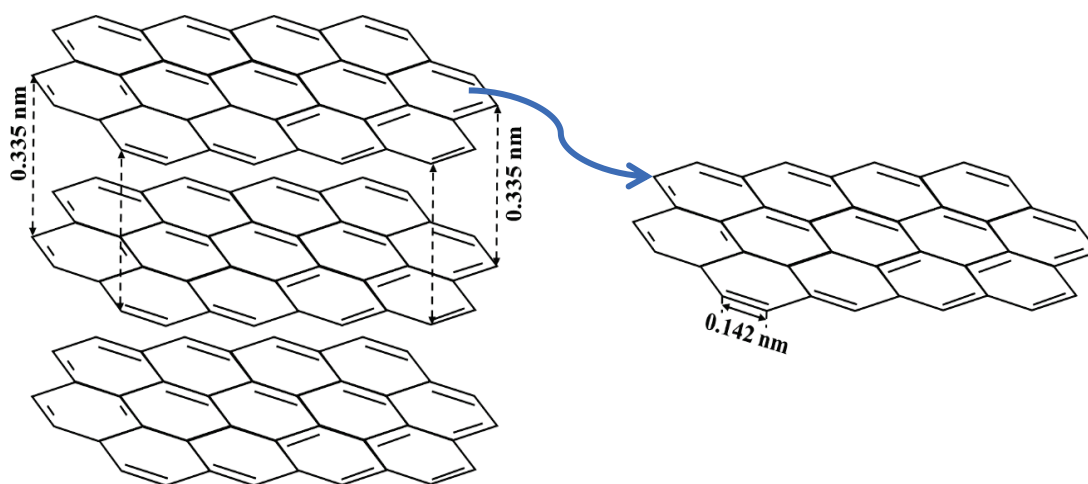
Figure 1. 5. Structure of graphite (left) and graphene (right)

Graphene has two-dimensional crystal structure formed by the arrangement of carbon atoms in a single plane with hexagonal matrix. The hexagonal structure of carbon atoms may provide exceptionally high electrical and thermal conductivity, robustness (100 times stronger than steel), flexibility, chemically low reactivity, high transparency, ferromagnetic properties at room temperature, and superconducting or semiconducting properties depending on the synthetic conditions. Electrons act as if they have no mass in this single atomic thickness graphene carbon layer, which shows its high electrical properties (Xiang, Yu, and Jaroniec 2012; Lu et al. 2009). The structure of graphene is single-atomic layers of densely packed carbon atoms in a honeycomb crystal structure.

Graphene oxide (GO) can be produced from graphite (Hummers and Offeman 1958; Park and Ruoff 2009). But different synthetic methods may result in varying degrees of oxidation (Krishnamoorthy et al. 2013). In general, the most common representative structure for the obtained graphene oxide is shown in Figure 1.6. The functional groups; hydroxyl (-OH), carboxyl (-COOH), carbonyl (-CO) and epoxy (-COC-) groups are present in the structure of GO (Lerf et al. 1998). Due to the presence of these functional groups GO shows a high degree of hydrophilic properties and also forms stable aqueous colloids. In addition, GO has electron acceptor and charge trapping properties. These properties are preferred in photocatalytic processes but are problematic for applications requiring electrical conductivity. Therefore, in those kinds of applications GO is converted to reduced graphene oxide (RGO) (Figure 1. 6) (Zainuddin et al. 2018) or modified with amine sources.
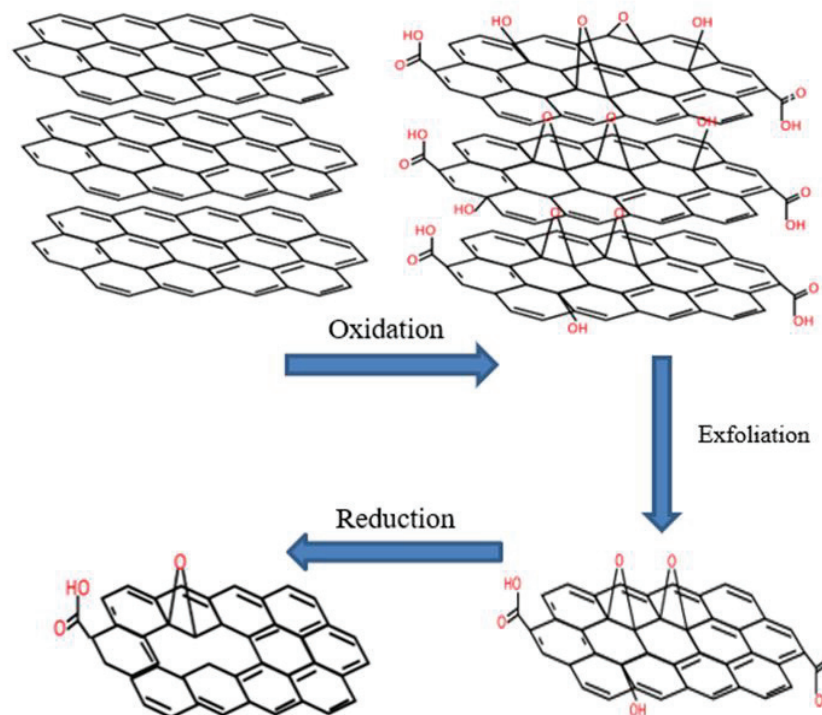
Figure 1. 6. Schematic representation of RGO synthesis from graphite.

Amin Modified Graphene Oxide (mGO); The term modified graphene oxide (mGO) represents the attachment of different organic or inorganic groups to the GO by chemical reaction. The main purpose of adding groups having different properties to GO is to increase the functionality of GO and thus to change its the electrical, structural and optical behavior (Zainuddin et al. 2018; Diker, Bozkurt, and Varlikli 2020). Methods used in obtaining mGO are summarized below:

Covalent modification is the modification by using the active double bonds and oxygenated functional groups. In the covalent modification of graphene, strong acids and radicals with high reactivity, containing hydroxyl, carboxyl and epoxy groups are used (Salavagione, Gómez, and Martínez 2009; S. Wang et al. 2008). The structural change achieved by covalent modification is carried out on the surface of the graphene layer. Surface functionalization is related to the re-hybridization of one or more sp^2 carbon atoms to the sp^3 configuration. These reactions may involve, nucleophilic displacement, electrophilic addition, condensation and/or addition polymerization. Modification with amine sources involves nucleophilic substitution and condensation reactions. Functional groups which react with amine groups in the GO layer are epoxy

groups in the basal region and carboxylic acid groups in the corner regions (Kuila et al. 2012; Wenjuan Li et al. 2011; Shanmugharaj et al. 2013).

Non-covalent interactions use hydrogen bonding, van der Waals interactions, $\pi - \pi$ stacking, electrostatic forces and coordination bonds and result with physical adsorption of suitable molecules on the graphene surface. In the non-covalent modification process, the structure and properties of graphene can be sufficiently preserved (Georgakilas et al. 2012). The use of $\pi - \pi$ interactions (stacking) is the most effective non-covalent modification method and may allow attaching the ionic liquids, macromolecules (Lonkar, Deshmukh, and Abdala 2015) as well as the inorganic compounds (Q. Yang et al. 2010). The entire surface of the graphene is easy and is reversible in some cases. However, the adsorption of materials to the graphene surface is not as strong as in covalent modification; when the external environment changes the complex becomes unstable (Georgakilas et al. 2016).

1.2.3. Graphene-TiO$_2$ Composites in Photocatalysis

In order to overcome the limitations of TiO$_2$ in photocatalytic activity and create more efficient catalyst, various modification methods have been designed so far (Table 1.1.). Among these methods, the combination of graphene and graphene derivatives with TiO$_2$ attract attention due to unique electrical and optical properties of graphene. In the literature, graphene based TiO$_2$ composites have shown remarkably improved photocatalytic activity in wastewater treatment and promoted as a potential photocatalyst for new future applications. The improvements in photocatalytic activity of TiO$_2$ are based on the approaches mentioned below:

- Modifying TiO$_2$ particles allows improving the surface area and adsorption capacity of the photocatalyst due to the strong and intimate interactions between them. The honeycomb two-dimensional crystal structure of graphene and graphene derivatives such as GO and RGO, is suitable host material for the dispersion of TiO$_2$ particles. The GO and RGO surfaces include functional groups, which allow the TiO$_2$ particles to be anchored on to the surface of them. In this way, the aggregation problem of TiO$_2$ nanoparticles is minimized and results in greater surface area. The adsorption of organic pollutants and

reactants is directly related to the increase in surface area of photocatalyst and plays an important role in the improvement of photocatalytic activity (F. Wang and Zhang 2011a).

- The enhancement of the photocatalytic performance of TiO_2 using graphene-based materials is based on improving charge separation and transport in the photocatalysts. Graphene has excellent mobility of charge carriers so it is an ideal material for charge trapping. Both of GO and graphene act as electron acceptors in their composites, providing higher charge separation. Moreover, the presence of carbon in their nature also increase light absorption in the visible region of solar spectrum. It is also reported that aromatic contaminants has shown better adsorption on the surface of carbon based photocatalyst due to the strong π–π interactions between the GO or graphene and contaminant (Rong et al. 2015; Sher Shah et al. 2012).

- Decrease of the rate of recombination of e- / h+ pairs has been reported after the combination of GO or reduced GO and TiO_2 in literature. The great electrical conductivity provided by π–π conjugated structure inhibits the recombination of photogenerated charges. In GO-TiO_2 composites, e- / h+ pairs are formed in TiO_2 when illuminated by UV light. These excited electrons tend to be transferred to the GO material. Dissolved oxygen in the medium also prevents recombination of the e- / h+. On the other hand, the photogenerated h+ can react with water molecules adsorbed to the surface to form hydroxyl radicals, or they can directly oxidize organic compounds. The reactions that occur in the photodegradation mechanism with Graphene-TiO_2 composite photocatalyst under UV light are briefly identified by the following equations [(2), (12)-(14)] (Xiang, Yu, and Jaroniec 2012).

$$TiO_2 + hv \rightarrow TiO_2 \qquad\qquad\qquad (2)$$

$$TiO_2(e^-) + graphene \rightarrow TiO_2 + graphene\ (e^-) \qquad\qquad\qquad (12)$$

$$graphene\ (\ e^-) + O_2 \rightarrow graphene + O_2\text{-}\bullet \qquad\qquad\qquad (13)$$

$$TiO_2(h^+) + OH^- \rightarrow TiO_2 + OH\bullet \qquad\qquad\qquad (14)$$
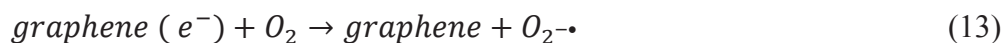
Table 1. 1. Results of photocatalytic degradation of GO-TiO$_2$ composites.

References	Photocatalyst	Dye	Time (min)	Light Source	Deg.%
(Jaihindh, Chen, and Fu 2018)	rGO/Ag/Fe/TiO$_2$	MB	150	Xe arc lamp	95.33
(Sohail et al. 2017)	rGO/TiO$_2$	MB	60	UV	92
	TiO$_2$				71
(Xiao et al. 2017)	rGO/Ag/TiO$_2$	MB	160	HP Hg lamp	100
(Wei et al. 2016)	Cu(II)-tetrakis(4-carboxyphenyl) porphyrin- rGO/TiO$_2$	MB	120	VIS	95
(Wan et al. 2016)	Porphyrin-rGO/TiO$_2$	MB	120	VIS (>390 nm)	92
(Rong et al. 2015)	Grafen-TiO$_2$	MB	100	VIS (>420 nm)	98.8
(Benjwal et al. 2015)	rGO/Fe$_3$O$_4$/TiO$_2$	MB	5	HPMV lamp	UV-100 Vis-91
(Wenqiang Li, Liu, and Li 2015)	Graphene/Fe–TiO$_2$	MB	80	VIS	99.5
(Ismail et al. 2013)	TiO$_2$/GO	MB	180	Halogen	98.5
(Gu et al. 2013)	rGO/TiO$_2$	MB	80	Hg lamp	98
(Yin et al. 2013)	N- rGO/NTiO$_2$	MB	160	Xe	80
	NTiO$_2$				60
(Yoo et al. 2011)	GO/TiO$_2$	MB	180	UV and fluorescent	UV-45 Vis-25
	GO				UV-30 Vis-20
(Yuan et al. 2005)	ZnCdS/TiO$_2$/RGO	MB	60	UV 365	100
(Cao et al. 2015)	rGO/TiO$_2$	MO	100	UV 254	96.4

Table 1. 1. Results of photocatalytic degradation of GO-TiO$_2$ composites (Cont.).

References	Photocatalyst	Dye	Time (min)	Light Source	Deg.%
(Pu et al. 2013)	GO/TiO$_2$	MO	40	UV 365	95
	TiO$_2$				90
(Khalid et al. 2012)	Graphene- NTiO$_2$	MO	175	VIS(>420 nm)	~100
	NTiO$_2$				50
(Gao et al. 2012a)	GO/TiO$_2$	MO	80	UV 365	~100
(Nguyen-Phan et al. 2011)	GO/TiO$_2$	MO	60	UV and Vis	UV-100
					Vis-75
	TiO$_2$				UV-40
					Vis-20
(Maruthamani et al. 2015)	rGO/TiO$_2$	RhB	300	UV 365	93.8
(F. Wang and Zhang 2011b)	rGO/ TiO$_2$	RhB	120	UV 365	UV-85 Vis-65
	TiO$_2$			VIS 420	UV-45 Vis-15
(Liu et al. 2013)	GO/TiO$_2$/Ag	AO 7	80	Sunlight	100
(Jing et al. 2014)	GO/TiO2	Quinolinee	120	UV 365	UV-100
					Vis-75
(Yu et al. 2019)	RGO/TiO$_2$	BisPhA	30	Sunlight	100

1.2.4. Perylene Derivatives in Photocatalysis

Dye sensitization appears to be a suitable and cost-efficient alternative method to increase photocatalytic activity and in particular to extend the activity towards the visible light field. To date, various types of dyes have been used as photosensitizers with TiO$_2$, which can be examined under three groups as xenene dyes, transition metal based dyes and organic dyes. The greater performances of the dye / TiO$_2$ systems are attributed to the fact that the dyes tested have higher oxidation potentials than that of

TiO_2, which makes it possible to transfer electrons from the excited state of the dye to the CB of TiO_2.

The xanthan dyes have low cost, large visible light absorption and moderate oxidation-reduction properties compared to the other dyes. However, they are not the most commonly used dyes to sensitize TiO_2 in practice, due to their lower photoconversion efficiency and poor chemical stability (Youssef et al. 2018).

Transition-metal-based sensitizers are the most popular among a variety of photosensitizers and are widely preferred in dye-sensitized solar cells. Transition metals such as Ru (II), Fe (II) and Os (II) form the d^6 complex and provide strong charge transfer absorption at the visible range. However, they are quite expensive due to the large cost of the synthesis and the purification steps and unfortunately not suitable to be used in water treatment because they are toxic (Wasylenko et al. 2012; Zhao et al. 2018).

Organic dyes represent the most commonly used sensitizer for photocatalytic applications in water treatment. The most popular examples are porphyrin, phthalocyanines and perylene dyes. Among them perylene derivatives are inexpensive organic dyes with strong absorption in the visible light region and large light absorption coefficient (C. Karapire et al. 2005; Kus et al. 2008; Canan Karapire, Zafer, and İçli 2004; Shang et al. 2011; Youssef et al. 2018). They exhibit high photo, chemical and thermal stability. Due to their structures, perylene dyes possess a low solubility in aqueous media. PTE is a typical perylene derivative with n-type semiconductor character with high electron affinity (lower LUMO level) and electron mobility due to its strong delocalized conjugated π bonds and carbonyls of the ester functional group. An electron can be transferred from the LUMO of PTE to the conduction band of TiO_2, and the hole can transfer from the valence band of TiO_2 to the HOMO of PTE. Based on this, PTE can be considered as an efficient candidate for visible-light sensitization of the TiO_2 composite and improve separation of photogenerated $e^- - h^+$ pairs.

In this study, newly synthesized mGO-TiO_2 and other photocatalysts were sensitized by PTE dye. The predicted photocatalytic mechanism and energy band diagram is shown in Figure 1. 7 and Figure 1. 8 .
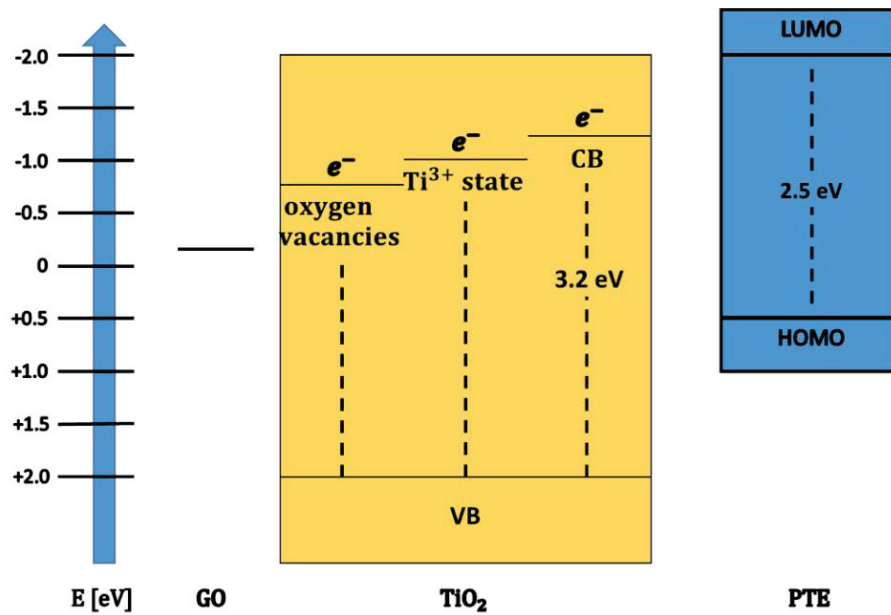
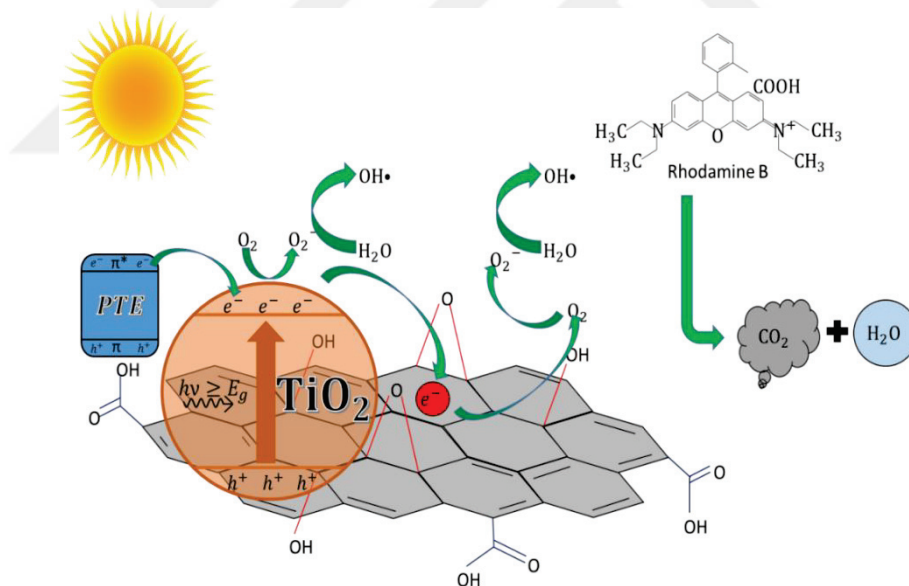Figure 1. 7. Energy band diagram of PTE/ GO:TiO$_2$ structure.

Figure 1. 8. Photocatalytic mechanism of PTE/mGO:TiO$_2$ structure.

1.2.5. Importance of light source in Photocatalysis

One of the most important factors affecting photocatalytic activity is the light source. The light provides the energy required for electron transfer from the valence

band to the conductive band of the photocatalyst. As already mentioned, the energy required depends on which photocatalytic semiconductor is used. The light source should be selected considering the energy requirement of the reaction to be performed. The same catalysts exhibit different photocatalytic activity under different light sources (Table 1.1) (Nguyen-Phan et al. 2011).

In the laboratory, artificial light sources and small water volumes are used in photocatalytic activity studies. High-pressure mercury (Hg), xenon (Xe) or fluorescent lamps are commonly used as light sources Sometimes suitable filters (365 nm or 420 nm) are adapted to these lamps also in order to determine photocatalytic activity effectively (Yuan et al. 2005; Jaihindh, Chen, and Fu 2018; Xiao et al. 2017; Gu et al. 2013; Pu et al. 2013; Gao et al. 2012a; Yin et al. 2013).

Direct sun light has the advantages of being available at any time of the day, not requiring any energy consumption and effort, and being free and green energy. It is thought to be a great source because of these features. Metal halogen lamps (MGH) are best artificial light sources that are known to simulate direct sunlight. However, they are not preferred in photocatalytic processes as they deviate from direct sunlight spectral distribution at a wavelength of about 400 nm.

1.3. The Aim of the Thesis

In the study, it is aimed to eliminate the limitations of TiO_2 mentioned above and fabricate visible light driven photocatalyst. To reduce the aggregation of TiO_2 and the quick recombination of electron - hole pairs, composite photocatalyst will be formed with GO which has excellent electrical and optical property. In order to achieve photocatalyst with reusability, they will be fabricated in film phase. Characterization of all materials by using X-ray diffraction method, X-ray photoelectron spectroscopy, and BET analysis techniques. The films will be sensitized with PTE dye in order to obtain more effective films in the visible region. The photocatalytic activity of the produced films (P25, TiO_2, N-TiO_2, GO:TiO_2, GO: N-TiO_2 and mGO:TiO_2) will be monitored in the degradation of RhB dye which simulates water pollution under direct sunlight and under Xe lamp.

CHAPTER 2

EXPERIMENTAL

2.1. Materials

TiO$_2$, N-doped TiO$_2$, GO:TiO$_2$ and GO:N-TiO$_2$ were synthesized in MSc thesis of Gamze Belkıs Durmaz Çaycı, graphene oxide (GO) and n-propylamine modified GO (mGO) synthesized in the Ph.D. thesis of Halide Diker and a perylene tetraester (PTE) derivative synthesized by Ph.D. student Erkan Aksoy were used (Cayci, 2016; Diker, 2017). Commercially Available TiO$_2$ (P25) was supplied from Merck and used as the reference. Ethyl cellulose and N, N- dimethylformamide (DMF), terpineol, isopropanol (IPA), ethanol (EtOH) solvents were purchased from Sigma Aldric. Rhodamine B (RhB) was obtained from Fluka and chloroform was from Isolab Chemicals. Distilled water is used trough out all experiments.

2.2. Synthesis of Graphene Oxide Supported TiO$_2$ Nanocomposites

The GO supported TiO$_2$ nanocomposites were prepared by following the literate reports with minor modifications (Cayci 2016; F. Wang and Zhang 2011a). Shortly summarizing; 6 mg of mGO was dispersed in 80 mL of DMF and 80 mL of IPA. Then 400 mg of TiO$_2$ powder was added into the overall mixture. The mixture was pre-stirred for 2 hours then placed in the heater and reflaxed at 120 °C, for 48h. The precipitate was filtered and washed with IPA several times, and finally dried at 100 °C in the oven. The resulting particles were designated as mGO:TiO$_2$. The same procedure was repeated for obtaining GO:TiO$_2$ and GO:N-TiO$_2$ particles by using 80 mL of DI and 80 mL of EtOH solvent system.

2.3. Preparation of TiO_2 Paste and TiO_2 Films

200 mg of each modified titania powder sample was dispersed in 1.6 mL of EtOH and grinded in a mortar. The dispersion is exposed to ultrasonic bath for 40 min. Ethyl cellulose (100 mg) was added in to the dispersion and stirred for 90 min. Finally, 0.3 ml terpineol was added. The resulting TiO_2 paste was coated on glass substrate by doctor-blade technique and allowed to dry at 500 °C by heat gun.

2.4. Instruments

XRD measurements were performed with a high resolution X-ray diffractometer (Philips X'Pert Pro) using Cu Kα radiation. Data sets were confined in the range of 0–80° (2θ) and the average crystallite size of nanoparticles was determined according to XRD results. The binding energy values were determined with Thermo K-Alpha Monochromated XPS spectrometer model. By the use of a Micromeritics Gemini V device and application of Brunauer Emmet and Teller (BET) method based on nitrogen (N_2) gas adsorption technique at 100 °C, specific surface area of the each sample was determined. The film thicknesses were determined by Kla Tencor IXL 100 optical profilometer and absorbance measurements for monitoring the photodegradation of RhB solution were performed with Edinburgh FS5 spectrofluorotometer. Intensity of Xenon lamp (Xe) (1000 W) and direct sun light were measured in terms of W/m^2 by the use of a solar power meter LA-1017. The intensity of Xe was determined as 190 ± 7 W/m^2 and direct sunlight was measured as 800 ± 45 W/m^2.

2.5. Photocatalytic Activity Studies

Photocatalytic activities of TiO_2 films (P25, TiO_2, $N-TiO_2$, $GO:TiO_2$, $GO:N-TiO_2$ and $mGO:TiO_2$) were investigated during photocatalytic degradation of RhB in water under Xe and direct sunlight. In order to analyze the photocatalytic effect of the films, the photodegredation of RhB dye without photocatalyst was also followed.

Prepared films were placed in 6×10^{-6} M RhB solution and were waited under dark for 24 h to provide adsorption desorption equilibrium. In order to study the photocatalytic activities of the films, the solution absorbance was measured with respect to radiation time of the photocatalyst. The TiO_2 films were further sensitized with PTE dye by soaking the films in 1×10^{-3} M PTE chloroform solution for 6h. After waiting for the films to dry in air conditions for 30 min. the procedure described for the non-sensitized films was repeated.

In order to test the reusability of the prepared films, photodegradation process was repeated using the same films three times. Before repeating photodegradation, all films were waited in DI for 24 h and PTE sensitized films were remained in chloroform solution for an additional 24 h. After that, non-sensitized films were dried at 100 °C and PTE sensitized ones were dried at 500 °C. Schematic representation of experimental setup used during the photocatalytic degradation experiments performed under Xe lamp is presented in Figure 2.1 :
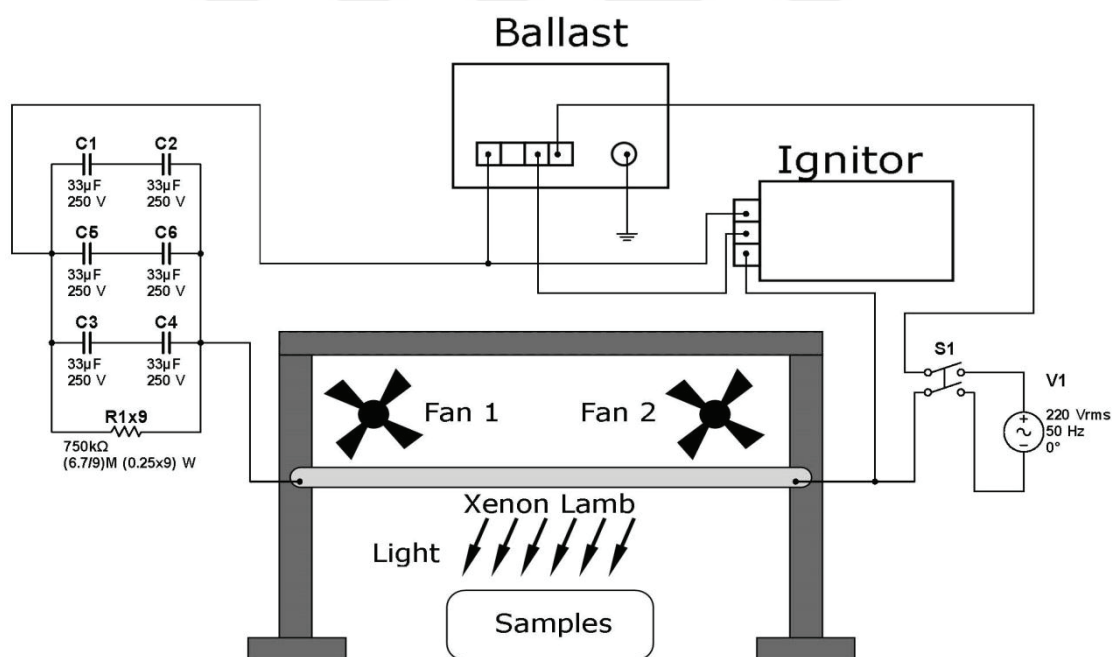

Figure 2.1. Experimental setup used during the photocatalytic degradation experiments performed under Xe lamp.

CHAPTER 3

RESULTS AND DISCUSSION

3.1. Characterization of the Photocatalyst

FT-IR spectra of $GO:N-TiO_2$, $GO:TiO_2$, $mGO:TiO_2$, $N-TiO_2$, TiO_2 and GO photocatalysts are given in Figure 3.1. The stretching peaks observed, confirm the existence of $C=O$ (~1720 cm^{-1}) and olefinic carbon (~1600 cm^{-1}) groups in the GO structure as discussed in literature (Maruthamani, Divakar, and Kumaravel 2015; X. Wang et al. 2016). The characteristic, alkoxy (~1050 cm^{-1}), epoxy (~1250 cm^{-1}) and carboxyl (~1400 cm^{-1}) peaks of GO are observed as broad peaks between 1490 cm^{-1} and 1000 cm^{-1}. This broad peak shifted to lower wavenumber in the $GO:N-TiO_2$, $GO:TiO_2$ and $mGO:TiO_2$ composites. This could be explained by the vibration of Ti-O-Ti and Ti-O-C bonds which formed due to the anchoring of TiO_2 onto the GO sheet through epoxy and hydroxyl sites (Khalid et al. 2012). Unlike the other photocatalysts, a sharp peak at 1385 cm^{-1} is observed for the $mGO:TiO_2$ composite. This peak is attributed to the C-C stretching of $C-(CH_3)_2$ groups of dipropylamine in GO structure whereas, the peak at 1120 cm^{-1} could correspond to the stretching vibrations of C-O and C-N bonds. The intensity of 1120 cm^{-1} peak was higher in N containing photosensitizers than those of the others and this is commentated as an indication of successful introduction of amine group in the GO structure. The C-H stretching and bending vibrations are observed at ~2900 cm^{-1} and 1460 cm^{-1}, respectively. Also, N-H bending vibration of amine group may have overlapped with the C=C stretching vibration of GO at ~1630 cm^{-1}. The potato like wide peak above 3000 cm^{-1} is attributed to stretching vibration of C-OH groups, which is consistent in the $GO:N-TiO_2$, $GO:TiO_2$ and $mGO:TiO_2$ spectra (F. Wang and Zhang 2011b). This peak of $mGO:TiO_2$ composite became much larger than those of the $GO:N-TiO_2$ and $GO:TiO_2$ composites. This can be explained by the overlapping of stretching vibrations of C-OH and N-H groups. The C=O bond stretching peak is disappeared in $GO:N-TiO_2$, $GO:TiO_2$ and $mGO:TiO_2$ structure because of the partial reduction of GO during the hydrothermal reaction.
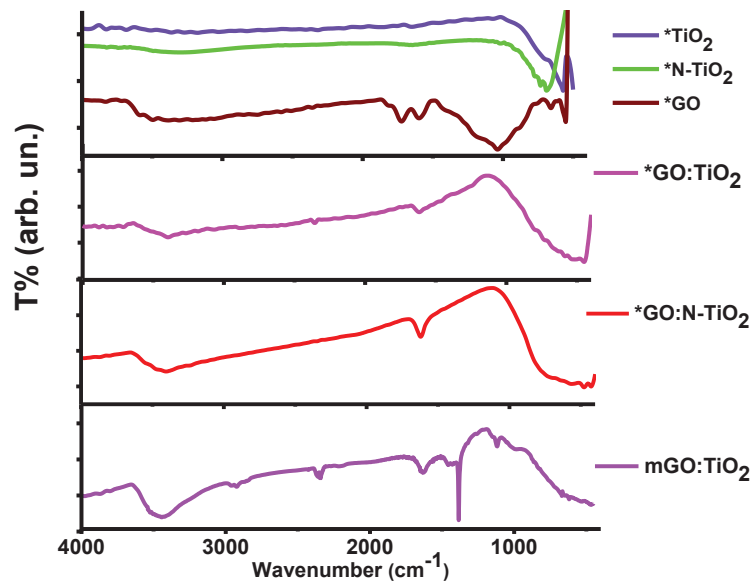
Figure 3.1. FT- IR spectrum of the photocatalysts. (* samples synthesized and analysed in MSc thesis of Gamze Belkıs Durmaz Çaycı (Cayci 2016))

The chemical states of elements in GO, TiO_2, N-TiO_2, GO:TiO_2, GO:N-TiO_2 and mGO:TiO_2 were analysed by XPS. Survey spectra of composites (Figure 3. 2) clearly indicate the existence of C, O, Ti and N in the materials, thereby implying that TiO_2 was successfully combined with GO and mGO.

The core-level XPS signals of Ti 2p are shown in Figure 3. 3 . The Ti 2p core level spectrum displayed two peaks which are located at the binding energies of 458.8 eV and 464.3 eV and correspond to Ti 2p1/2 and Ti 2p3/2 spin orbital splitting photoelectrons in the Ti4+ chemical state, respectively (Cruz et al. 2017). No significant difference between the photocatalysts could be detected and this situation is interpreted as the indication of strong interaction between TiO_2 and GO.

The O 1s XPS spectra of all photocatalysts are shown in Figure 3. 4 . The two peaks centred at binding energies of 531.5 eV and 532.5 eV are assigned to the C-O, C=O and C-OH bonds originating from different functional group types such as hydroxyl, epoxy, carbonyl and carboxyl groups of GO (D. Yang et al. 2009). Whereas, the binding energies of 530 and 532 eV observed in GO /TiO_2 composites are attributed the lattice of oxygen in TiO_2 (Ti-O bond) and –OH groups on the surface of TiO_2 (Tan et al. 2015), respectively.
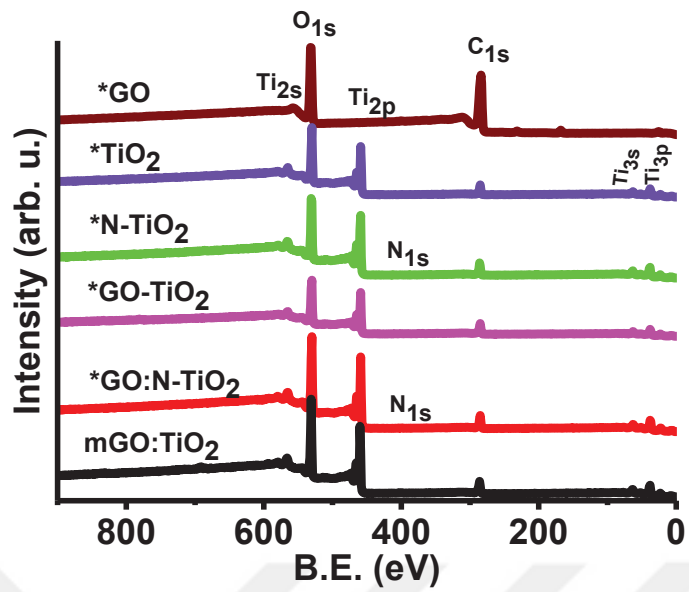
Figure 3. 2. General elements spectrum of the catalysts. (* samples synthesized and analysed in MSc thesis of Gamze Belkıs Durmaz Çaycı (Cayci 2016)).
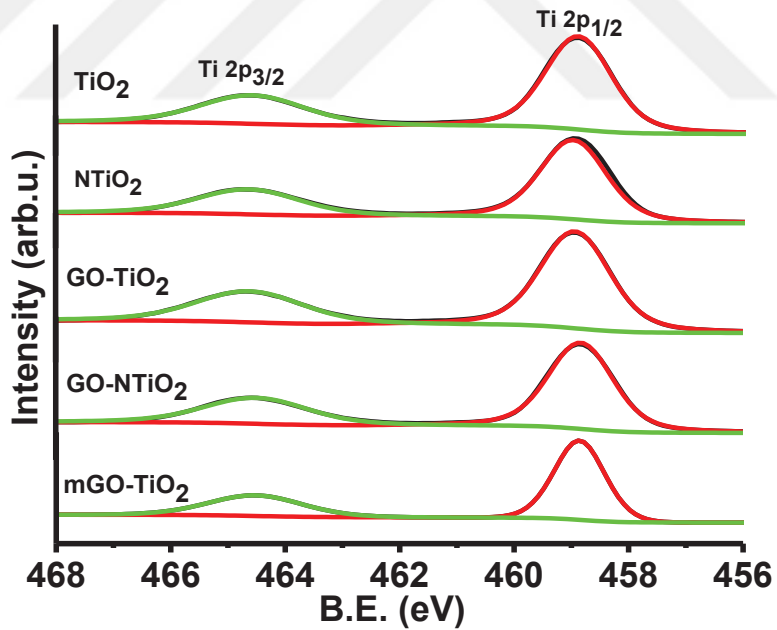

Figure 3. 3. Ti 2p spectrum of the catalysts. (* samples synthesized and analysed in MSc thesis of Gamze Belkıs Durmaz Çaycı (Cayci 2016)).

The core-level XPS signals of C1s shown in Figure 3. 5 . As for GO, the primary peak was obtained at 284.4 eV, which is related to the C-C bond in sp2 hybridization. Beside the peak at 284.4 eV, the peaks located at 286.2 eV and 288.5 eV are attributed to C-O of epoxy / hydroxy and O-C=O of carboxyl and carboxylates groups (Yin et al. 2013). After the composite formation of GO and TiO_2, it was observed that the intensity of the oxygenated functional groups are decreased compared to that of the GO sample which generate from the residual oxygenated groups remaining on the GO / TiO_2 composites. The peak at 287.9 eV (O-C=O bond) is shifted to higher energy 288.9 eV (Ti-O-C bond), resulting from the coordination bond between Ti and carboxyl acids on the GO during the composite preparation (Zhang and Pan 2011).
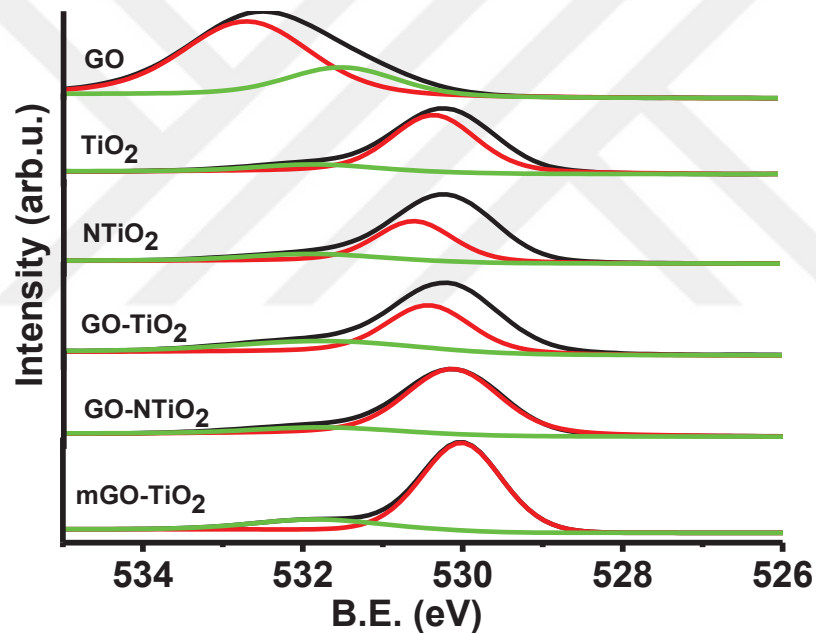

Figure 3. 4. O1s spectrum of the catalysts. (* samples synthesized and analysed in MSc thesis of Gamze Belkıs Durmaz Çaycı (Cayci 2016)).

Furthermore, based on the XPS results of C 1s spectra, the peak area ratios of the C-O, C=O, and C-C bond were calculated and summarized in Figure 3. 6. The remarkable decrease in the % of the oxygen containing functional groups and increase in the % of C-C of GO are interpreted as effective reduction of the GO in the composite. The oxygen-containing species on the surface of the photocatalyst has the potential of

enhancing the dye adsorption capacity of catalyst and thus increasing the photocatalytic activity.
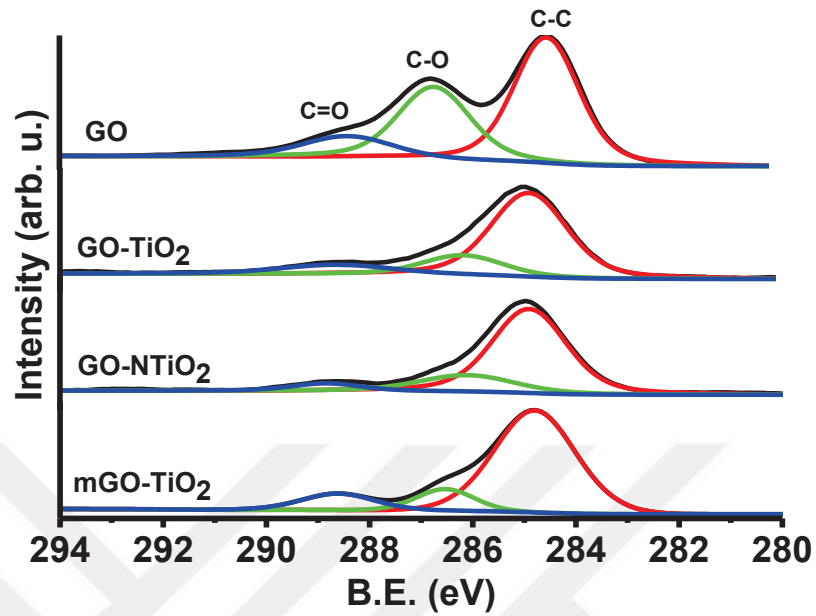

Figure 3. 5. O1s spectrum of the catalysts. (* samples synthesized and analysed in MSc thesis of Gamze Belkıs Durmaz Çaycı (Cayci 2016)).
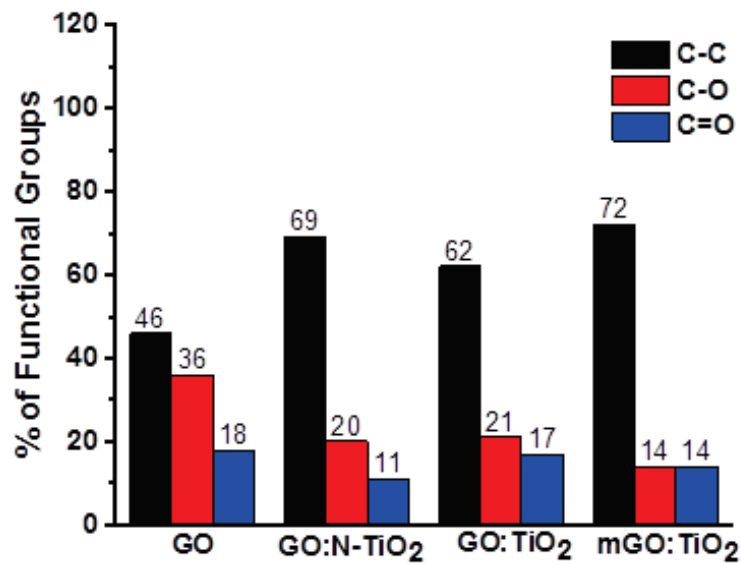

Figure 3. 6. The peak area ratios of the C-O, C=O, and C-C bonds in the structure.

X-ray diffraction spectroscopy is a technique mostly used to determine crystal phase properties and average crystalline size. Figure 3. 7 indicates the XRD patterns of all photocatalysts used in this study. Previous studies have shown that the 2θ characteristic peak for the graphite is $26°$ and when the graphene is oxidized to graphene oxide this value shifts to $8°$-$10°$ (Fu et al. 2013). In this study, the 2θ peak of GO was observed at $10°$ along with a shoulder at ~$24°$. (Figure 3.7 inset). In literature, 2θ peak of $24°$ is attributed to reduced GO (Fulari et al. 2018). As stated in Gamze Belkıs Durmaz MSc Thesis (Cayci 2016), drying process at 100 °C was employed as the final step of GO preparation. It is thought that some of the functional groups may have been removed while the others remained in the structure during this process. In all TiO_2 containing samples, the most intense peak is detected at $2\theta = 25°$ indicating the anatase phase of TiO_2. The $10°$ peak is not observed in GO:N-TiO_2, GO:TiO_2 and mGO:TiO_2 composites due to partial reduction of GO during the hydrothermal reaction whereas, secondary peak of GO was overlapped with the anatase phase peak (J. Wang et al. 2016; Khalid et al. 2012). Therefore, the GO / TiO_2 composites displayed a diffraction pattern similar to that of bare TiO_2. The modified-TiO_2 crystal structures are determined using XRD characterization device and the particle size is calculated from Scherrer equation (Shao, Zhang, and Yuan 2008).
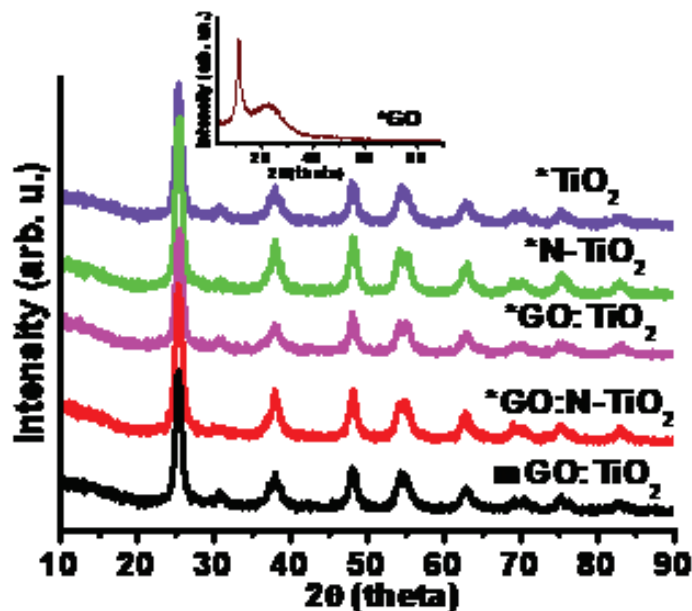

Figure 3. 7. XRD patterns of the catalysts. (* samples analysed in MSc thesis Gamze Belkıs Durmaz Çaycı (Cayci 2016)).

Crystalline size of the photosensitizers are calculated from Scherrer equation (Patterson 1939)

$$\text{Scherrer equation,} \quad D = \frac{K \times \lambda}{\beta \times \cos\theta}$$

where D is the mean size of crystallites (nm), K is crystallite shape factor (a good approximation is 0.94), λ is wavelength, β is the full width at half the maximum in radians of the X-ray diffraction peak and Θ is the Bragg's angle. Calculated crystal sizes of all samples are provided in Table 3.1. Crystal sizes of GO based TiO_2 reported in the literature range from 10 nm to 20 nm. In this study, the D values of the used photocatalysts changed between 13.1 – 8 nm. The sizes of N-TiO_2 and TiO_2 samples are calculated to be 11 nm. After composite formation with GO, the D value decreased to 8 and 8.8 nm for GO:N-TiO_2 and GO:TiO_2 samples, respectively. This decrement is attributed to the sheet like exfoliated structure of GO (Figure 3. 8 a) which acts as a plane substrate for the N-TiO_2 and TiO_2 particles. Whereas, the dot like morphology of mGO (Figure 3. 8 b) is assumed to induce a slight increment in the D value of mGO:TiO_2 (13.4 nm). Sheet and dot like structures of GO and mGO are clearly observed from the AFM images provided in Figure 3. 8 .
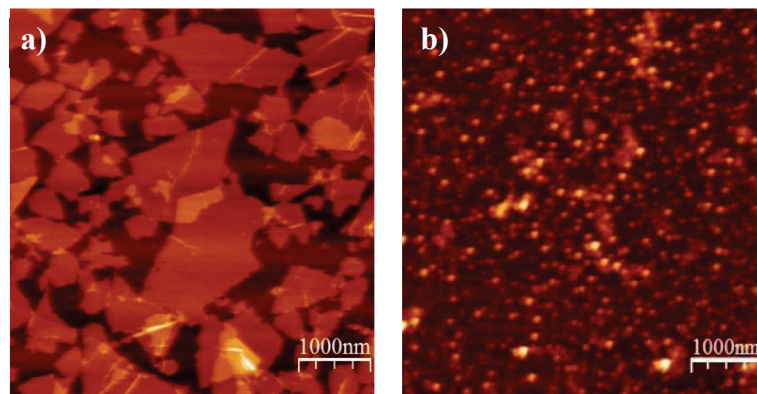

Figure 3. 8. AFM images of a)GO and b) mGO ("m" refers modification with dipropylamine and both of the images are taken from the PhD thesis of Halide Diker) (Diker 2017).

This assumption is further supported by BET characterization method as it provides information on the surface area. BET surface area measurements of prepared GO/TiO$_2$ composites in the study are summarized in Table 3. 1. Previous reports have indicated that BET surface area tends to increase after composite formation due to effective dispersion of TiO$_2$ nanoparticles in the GO host material. GO is stated as a good matrix to minimize the aggregation of TiO2 nanoparticles (Cao et al. 2015). Besides, the decreasing trend of specific surface area is also explained with agglomeration of GO in the composite, which occurs at high concentrations of GO during the hydrothermal treatment (Alazmi et al. 2016; Cruz et al. 2017). The surface areas of GO: TiO$_2$ and mGO: TiO$_2$ samples were 79 and 56 m/g, respectively and presented lower values when compared to that of bare TiO$_2$ (93 m/g). The same situation was valid for the N-doped photocatalysts; the surface area of N-TiO$_2$ (111 m/g) was higher than that of GO:N-TiO$_2$ (104 m/g). The dramatic decrease measured for the mGO:TiO$_2$ photocatalyst is attributed to the increased agglomeration, induced by the dot like morphology of amine functionalized GO sheets.

Table 3. 1. Specific surface area (SSA) and crystal size values of modified-TiO$_2$ particles. (* samples analysed in MSc thesis Gamze Belkıs Durmaz Çaycı (Cayci 2016)).

Sample	mGO:TiO$_2$	*GO:N-TiO$_2$	*GO:TiO$_2$	*N-TiO$_2$	*TiO$_2$	P25
D (nm)	13.1	8	8.8	11	11	13
SSA (m^2/g)	56	106	79	111	93	35

Photocatalytic activity of a photocatalyst is highly dependent on its particle size and surface area. In particular, catalysts having a large surface area and small particle size are expected to present higher activity (Pastrana-Martínez et al. 2012). However, as there are many other factors that affect the photocatalytic activity, literature contains some studies which have reported that smaller particle size materials do not always show high photocatalytic activity (Gao et al. 2012b). In the present study, GO:N-TiO$_2$ presents the smallest particle size and a lager surface area compared to those of GO:TiO$_2$ and mGO:TiO$_2$, which constitutes the expectation that photocatalytic activity of GO:N-TiO$_2$ will be higher than the others.

3.2. Photocatalytic Activity Studies

As stated at the experimental part, photocatalytic activities of fabricated films were observed under Xe lamp and direct sun light irradiation. Photocatalytic activities of the photocatalysts were compared by the use of first order kinetics and degradation rate constants were calculated by using the following Pseudo equation (Cao et al. 2015):

$$Ln \frac{c_0}{c} = kt$$

where C_0 is the initial concentration of the dye (Rh B), C is the concentration of the dye at time t and k is the rate constant. The absorption decrements at 559 nm, resulting from the degradation of Rh B were monitored for both with and without catalyst conditions (Rh B photocatalytic degradation without catalyst conditions under Xe lamp and direct sun light are given in Appendix A.). Before starting the photocatalytic studies, the films were dumped in the dye solution to establish adsorption-desorption equilibrium under dark condition as seen in Figure 3. 9.

The calculated number of adsorbed RhB molecules per volume of the films (#of RhB molc./V_{film}) (Table 3.2) was higher in the GO/TiO$_2$ composite photocatalysts and GO:N-TiO$_2$ adsorbed approximately 3 fold of dye molecules on its surface compared to those of regular TiO$_2$ nanoparticles. After N doping, the SSA of the catalyst increased and the particle size didn't change comparing to bare TiO$_2$. As a result of this, it allows adsorption of more dye molecule to its surface. However, contrary to the expected trend, the SSA decreased as a result of modification of TiO$_2$ with GO. Despite the decrease in the SSA, the number of dye molecules adsorbed onto the surface has increased and photocatalytic activity of GO – TiO$_2$ / N-TiO$_2$ also improved. In the presented study, it has also been proven that catalysts with smaller particle sizes and higher SSA do not always show high photocatalytic activity and surface modification plays significant role in photocatalytic activity. When composite photocatalysts are compared, the trend was in good accordance with the SSA values reported in Table 3.1; mGO:TiO$_2$ has higher particle size and smaller SSA, resulting in less dye molecules in composite catalysts.

Table 3. 2. Several parameters and the number of adsorbed RhB molecules per volume.

Photocatalyst	$A_0 - A_t$	#of RhB molc. ($\times 10^{14}$)	V_{film} (cm^3) $\times 10^{-4}$	#of RhB molc./V_{film} ($\times 10^{17}$)
mGO:TiO$_2$	0.067	37.583	26.05	14.43
GO:N-TiO$_2$	0.109	61.145	27.4	22.32
GO:TiO$_2$	0.093	52.183	28	18.64
N-TiO$_2$	0.052	29.151	29.25	9.97
TiO$_2$	0.039	21.875	28.7	7.62
P25	0.034	19.08	30.1	6.34

3.2.1. Under Xe Lamp Irradiation

Photocatalytic degradation performances of the used photocatalysts under Xe lamp irradiation are provided in Figure 3. 9 (related graphics of absorbance vs wavelength are given in Appendix B). Among them, GO:N-TiO$_2$ exhibited the best photocalytic activity and it degraded almost all Rh B in 300 min. The photocatalytic activity order of the prepared photocatalysts under Xe lamp is as follows:

GO:N-TiO$_2$ > GO:TiO$_2$ > N-TiO$_2$ > mGO:TiO$_2$ > TiO$_2$ > P25

Generally speaking, composite catalysts exhibited better photocatalytic activity. However, although the photocatalytic performance of mGO-TiO$_2$ is detected to be higher than bare catalysts, it presented the lowest performance within the composite catalysts including N-TiO$_2$.

In a study, Ramesha et al tested the adsorption capacity of graphene and GO on different dyes such as methylene blue, methyl violet, Rh B. According to their results, GO has a negative charge due to the hydroxylic and carboxylic groups present in the structure and thus showed very good adsorption ability by interacting with cationic dyes (Ramesha et al. 2011). The decrease in the ability of mGO to adsorb the dye is assigned to the reduction of the carboxylic and hydroxylic groups in the structure. The results of XPS analysis supported this situation. Figure 3. 6 shows the percentage of functional groups containing oxygen in the structure of GO and composite materials. The mGO: TiO$_2$ has less functional groups containing oxygen among other composites and the percentage of C-C increases, which inferred to reduction of GO in the structure. In

another evidence, the N-TiO$_2$ catalyst exhibited photocatalytic activity lower than GO-TiO$_2$ but greater than mGO-TiO$_2$ (GO: TiO$_2$> N-TiO$_2$> mGO: TiO$_2$). As it is known, N-TiO$_2$ is excited by visible light from the energy level which is a mixture of O 2p and N 2p orbitals formed after doping (Diker, Varlikli, and Stathatos 2014). Considering that the photodegradation starts with the adsorption of the dye on the surface of the catalyst, the amount of dye adsorbed on the surface is one of the most important parameters affecting the photodegradation. Based on this information, it is thought that the disappearance of hydroxylic and carboxylic groups on the GO surface as a result of mGO formation reduced its photocatalytic activity.
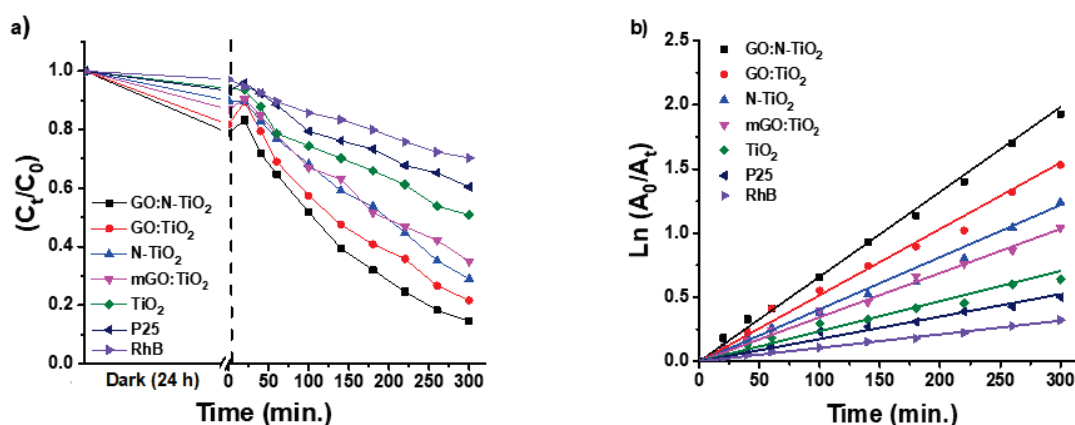

Figure 3. 9. a) RhB photocatalytic degradation by non-sensitized photocatalysts under Xe lamp irradiation and b) related rate constants of the reaction.

After the composite formation of GO with TiO$_2$ and N-TiO$_2$, photocatalytic activity was significantly increased. In the literature, the combination of TiO$_2$ with GO has been found to improve the surface area and adsorption capacity of the photocatalyst, and minimize the aggregation of TiO$_2$ nanoparticles (Sher Shah et al. 2012; F. Wang and Zhang 2011a). With these properties, GO can be widely used as a photocatalytic supporter for TiO$_2$ to develop the photocatalytic activity. There is a study performed by Vallejo et al. on graphene-TiO$_2$ composites to study the photocatalytic degradation of MB. They obtained the degradation yield 98% and yield 87.19% for MB under UV and visible light irradiation respectively (Vallejo et al. 2019). They reported that this activity was achieved because of the large surface area, providing a greater number of active surfactants in the materials. Therefore, the responsibility for enhanced photocatalytic

activity of GO-TiO$_2$ composites can be ascribed to loading of TiO$_2$ on GO sheets with large surface area. The GO sheets provide host material for dispersion of TiO$_2$ nanoparticles effectively and thereby minimize aggregation. The GO π-π conjugate structure also gives the electron acceptor properties and increases photocatalytic activity by preventing the recombination of the electron-hole in charge transport between the surfaces. XPS characterization results confirm the formation of composites with GO / mGO and TiO$_2$, and the results of photocatalytic activity studies support that TiO$_2$ is a great strategy to decorate with GO to develop effective photocatalyst. The lower performance of mGO may also be attributed to the presence of amine functional groups in the structure. The electrons from TiO$_2$ may be trapped and have negatively affected the formation of the superoxide radicals which is also responsible in oxidation-reduction.

Additionally, semiconductors can be bonded to these regions from the functional groups on the GO surface and from the defects caused by acidic species in chemical synthesis from graphite. After the low temperature hydrothermal reaction between GO and TiO$_2$, the covalent Ti-O-C bond is formed. This shifts the absorption of TiO$_2$ into the visible region and also increases the photocatalytic effect. There is some studies noted that Rh B may be adsorbed from both the GO and TiO$_2$ moieties and therefore the structures with GO: N-TiO$_2$ and GO-TiO$_2$ exhibit higher photocatalytic activity than the others (Khalid et al. 2012).

In the study, GO:N-TiO$_2$ film showed the best photocatalytic performance and this situation is expected when compared with GO:TiO$_2$ as well. The fact that N-TiO$_2$ is inducible by visible light affects photocatalytic activity. However, N-TiO$_2$ exhibited lower photocatalytic activity than these composites and higher photocatalytic activity than mGO:TiO$_2$, which adsorbs the least amount of dye on their surface (GO: N-TiO$_2$ > GO:TiO$_2$ > N-TiO$_2$ > mGO:TiO$_2$). The parameter that becomes apparent here is the large surface area results in more amount of dye attached on the surface and hence enhance the photocatalytic activity directly. Moreover, Khalid et al. measured PL intensity of TiO$_2$ and its composites and the results showed that among all the catalysts used in their study, pure TiO$_2$ indicated highest PL intensity and the emission intensities significantly weakened with N doping and graphene introduction. PL intensity is the result of recombination e - h pairs and lower PL intensity may indicate low probability of e - h recombination. Hence, among all samples, GO:N-TiO$_2$ exhibited the best photocatalytic activity, implying that the charge carriers were separated more

effectively due to the cooperative effect of N doping and composite formation with GO in the study.
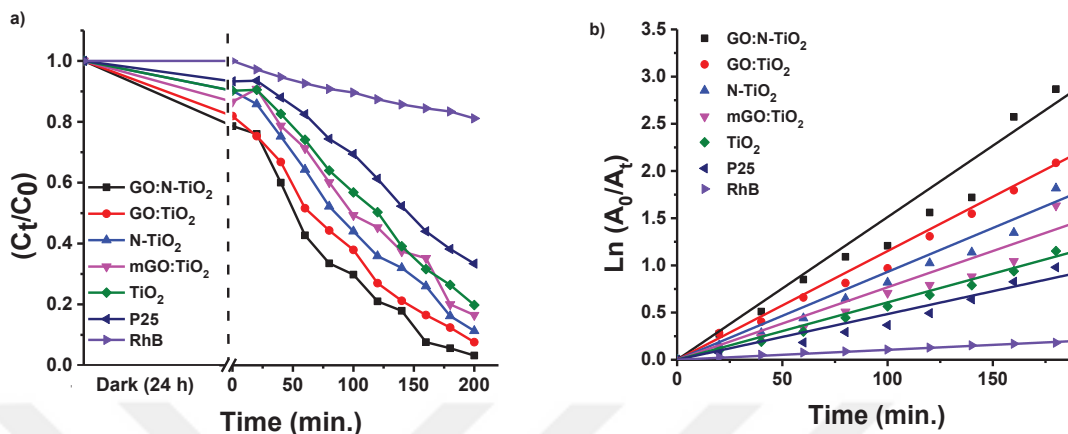

Figure 3. 10. a) RhB photocatalytic degradation by PTE sensitizied photocatalyst under Xe lamp irradiation and b) related rate constants of the reaction.

Perylene dyes are known as cheap organic dyes with high absorption coefficients, high electron affinities and electron mobilities due to their delocalized π electron system. At this stage of the study, PTE, a perylene derivative is introduced in the photocatalytic process with the motivation of enhancing visible light absorption and charge transport. All results indicated that PTE dye sensitization improved the photocatalytic activity of the fabricated films under Xe lamp; photodegradation rate constants were increased by a factor of 2. The best photodegradation activity was obtained by $GO:N-TiO_2$, showing that the presence of GO has an important role in combination with the dye sensitizer and TiO_2. GO can improve electron transport from sensitizer to TiO_2 and also reduce the electron hole recombination. Finally, all results corroborate that PTE dye are an economic, harmless and practical to be used in dye sensitization. The photocatalytic activity results of dye sensitized TiO_2 composites under Xe lamp are shown in Figure 3. 10 (related graphics of absorbance vs wavelength are given in Appendix C) and it is obvious from the Figure 3. 10 , PTE dye sensitized TiO_2 films and its composites exhibited greater photocatalytic activity than non-sensitized TiO_2 films. Although the order of photocatalytic activity did not change, the photocatalytic rate constants were significantly different. Rate constants have been

doubled for composite films and tripled for others. Table 3.3 summarizes the photocatalytic rate constants.

Table 3.3. The photocatalytic rate constants calculated as a result photocatalytic activity with Rh B.

Rate constants (x 10^{-3}) min^{-1}							
		GO:N-TiO$_2$	GO-TiO$_2$	N-TiO$_2$	mGO:TiO$_2$	TiO$_2$	P25
Non-sensitized	1. cycle	6.48	5.06	3.97	3.47	2.25	1.73
	2. cycle	6.3	4.96	3.91	3.39	2.08	1.72
	3. cycle	6.28	4.21	3.54	3.11	1.89	1.68
PTE-sensitized	1.cycle	15.12	11.52	9.31	7.68	6.08	4.84
	2. cycle	14.73	11.36	8.61	7.1	6.25	4.7
	3. cycle	12.44	9.54	8.29	6.95	5.63	4.64

The disadvantage of using the photocatalyst in suspension is the difficulty in separating from the reaction medium. To overcome this disadvantage, the photocatalysts were produced in film phase. The main aim of using the film form is eliminating the need for a costly extra-final filtration process, which is particularly important for water decontamination. Photocatalytic activity studies were repeated with the same films under the same conditions. Figure 3. 11 (related graphics of absorbance vs wavelength are given in Appendices D-G) demonstrate decomposition of Rh B which carried out with the same films for the second time and third time. No significant decrease in photocatalytic activity was observed in both dye sensitized films and composite films. It can be seen from Table 3.3 that the degradation rate constants slightly decrease after second and third utilizations and therefore fabricated films have suitable reusability. The slightly efficiency reduction in the degradation of Rh B may be caused by the loss of catalytic nanoparticles with the capability to keep unattached in films.

The photocatalytic films herein described is eco-friendly, cost-effective, and reusable for the treatment of contaminated water. More importantly, the produced photocatalytic films showed suitable reusability which has fundamental importance for an economical scaling-up system.
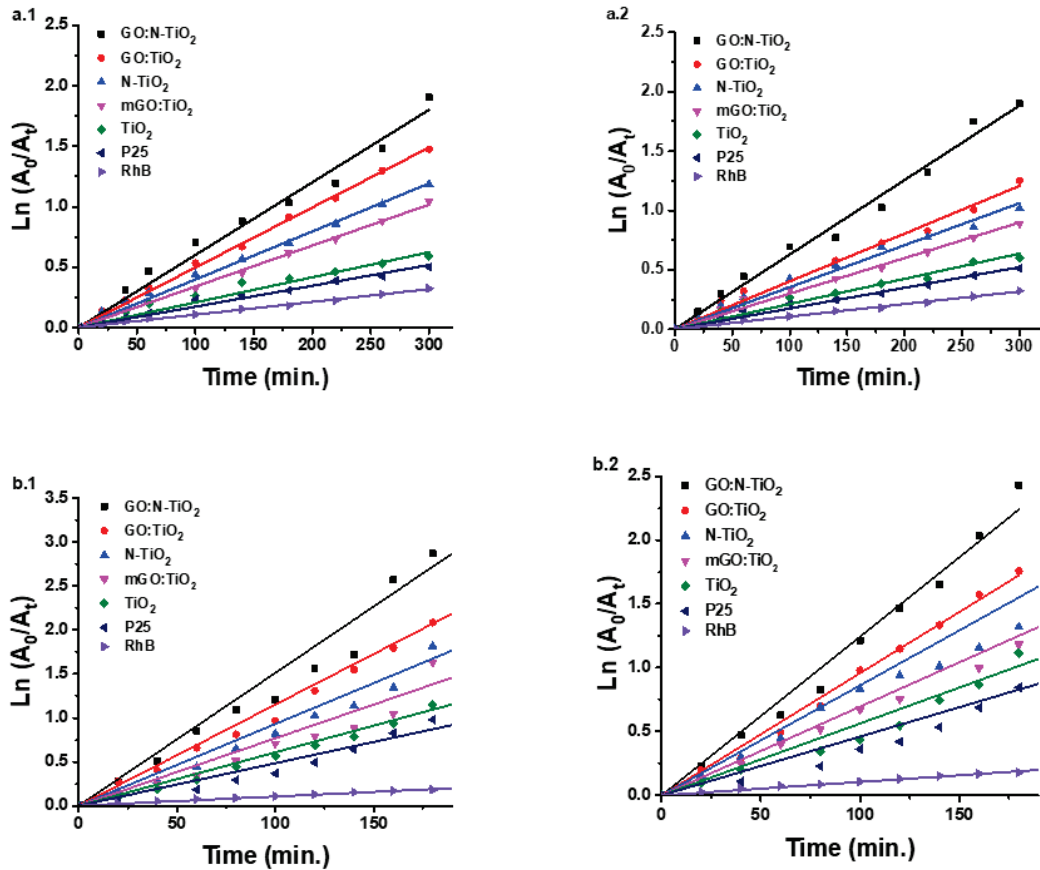

Figure 3. 11. Photocatalytic activity repeated for the second time and third time by a) non-sensitive photocatalysts and b) PTE dye - sensitized photocatalysts.

In the previous section, a theoretical scheme of energetic levels was proposed for the mGO-TiO$_2$ thin films with PTE sensitization. The mechanism of the photocatalytic degradation of the RhB dye of mGO:TiO$_2$ composite can summarize briefly; In the first stage, PTE dye absorbs the visible light and it is excited to a state of greater energy, leaving a hole in HOMO and an electron in the LUMO. This electron can be transferred to the conduction band of TiO$_2$. The electrons of TiO$_2$ are excited by the effect of UV light as well. These excited electrons are also transferred to electron acceptor GO due to its $\pi - \pi$ conjugate structure. At this point, GO act as electron traps

and inhibit the recombination process and GO's large surface area, keeps impurities on the surface and contributes to the acceleration of the photocatalytic process. The electrons localized in CB of TiO_2 or GO can be transferred to an oxygen molecule to produce superoxide anion. On the other hand, the photogenerated h+ can react with water molecules adsorbed to the surface to form hydroxyl radicals, or they can directly oxidize organic compounds. More reactive oxygen species and hydroxyl radicals can be generated and the degradation of pollutant begins. This process continues until there is no pollutant in the environment.

Moreover, Ti-O-C bonds formed between GO and TiO_2 are effective in the absorption of visible light. With all these effects, light absorption shifts to the visible region and photocatalytic efficiency increases.

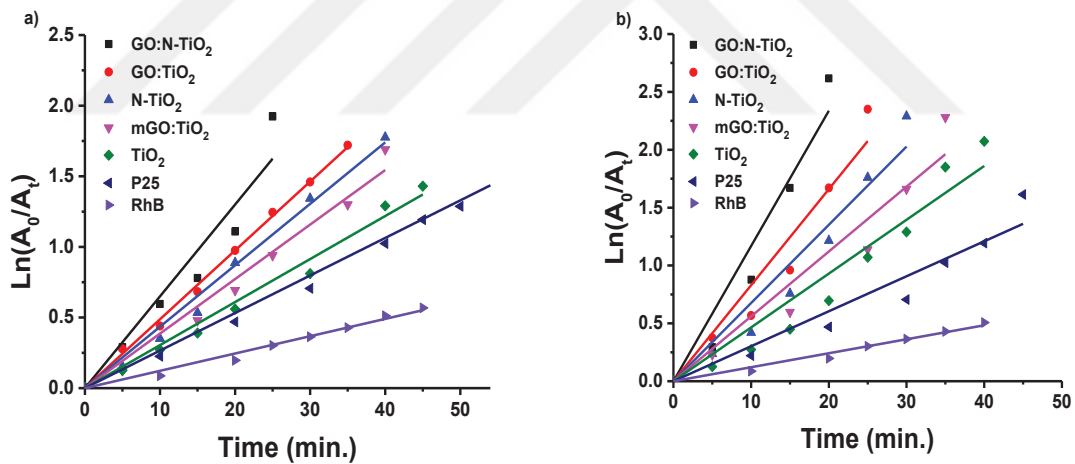## 3.2.2. Under Direct Sun Light Irradiation

Figure 3.12. a) RhB photocatalytic degradation non-sensitized TiO_2 films and b) PTE dye-sensitized films under direct sun light.

Multiple parameters such as surface area, particle size, surface hydroxyl groups, light source and intensity are also effective in photocatalytic degradation (Hudaya 2008; Diker, Varlikli, and Stathatos 2014). Of these, the light source plays one of the most important roles. Photocatalysts exhibit different photocatalytic performance with different light source and intensity. This shows us that different photocatalytic processes take place under different light sources. Photocatalysts need light radiation with a

threshold wavelength to promote electrons to the excited state. This threshold wavelength is dependent on the optical band gap of the photocatalyst: for example TiO_2 anatase with a band gap energy of 3.2 eV, it is about 387.5 nm, and thus it can only be excited by UV light which covers 4% of the solar spectra (Figure 3. 13 shows the Xe lamp and direct sunlight spectrum used in the study.). Therefore, it is highly desirable to develop visible light driven photocatalyst to overcome photocatalytic limitations. With this aspect, variety research efforts have been put into extending absorption of TiO_2 into visible region. Among these, the dye sensitization of TiO_2 nanoparticles has been proven to be one of the easiest and practical approaches for utilizing visible light which covers ~44% of the solar spectra. However, most reported photosensitizing dyes suffer from disadvantages such as expensive, thermally unstable, photobleaching, limited visible-light response or difficult functionalization (Chowdhury, Malekshoar, and Ray 2017).
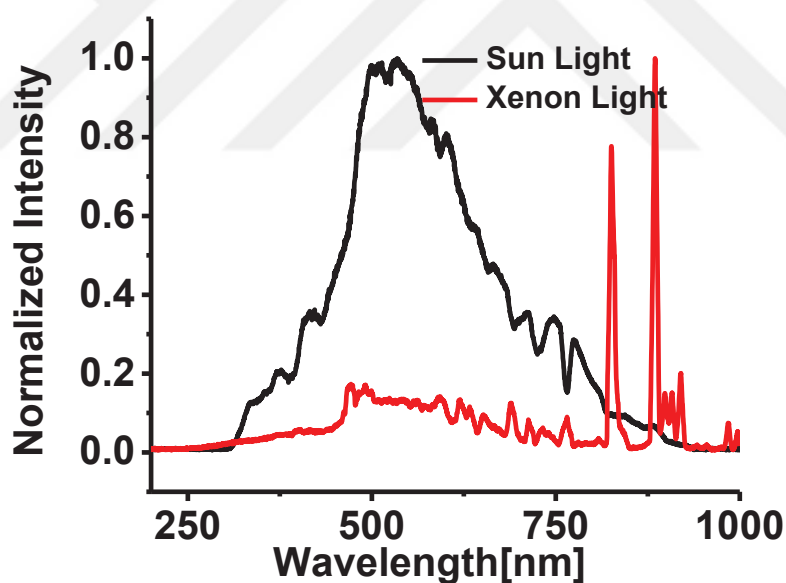

Figure 3. 13. Xe lamp and direct sunlight spectrum.

In this study, perylene dye was used as sensitizer by combining with GO /TiO_2 nanoparticles to increase photocatalytic activity in the visible region. Figure 3.12 shows the results of photocatalytic activity performed under direct sunlight for all films fabricated (related graphics of absorbance vs wavelength are given in Appendix H and I). Compared to photocatalytic studies performed with Xe lamp, the photocatalytic

activity was performed very fast and Rh B dyestuff was completely decomposed under direct sun light. Increase in photocatalytic rate constants of both PTE sensitized films and non-sensitized ones were observed but the PTE/GO/TiO$_2$ composites exhibit a better visible-light response. It can be attributed that PTE has energy levels at the positions of -3.27 eV and -5.77 eV for the HOMO and the LUMO, respectively, according to electrochemical cyclic voltammetry (CV) measurement. This ensures its visible-light absorption corresponding to a bandgap of 2.5 eV and its well matched energy levels to TiO$_2$. Further, the photocatalytic activity may be increased due to the strong electron-donor feature of PTE, constructing fast intermolecular charge transfer to TiO$_2$ unit (Shang et al. 2011). Under visible-light illumination, photoexcitation of PTE promotes electron transition to the LUMO and transfers it to CB of TiO$_2$, which ensure effective charge transfer among the PTE/GO/TiO$_2$ composite, degreasing electron-hole combination and enhance the photocatalytic activity as well.

The increase in photocatalytic activity of the non-sensitized films was also observed and the order of photocatalytic activity was not changed. The unchanged order and better photocatalytic performance of the composites can be attributed to the strong interaction Ti-O-C bond formed between the GO and TiO$_2$ mentioned above. With this bond, the absorption of TiO$_2$ shifts to the visible region and thus increases the photocatalytic activity.
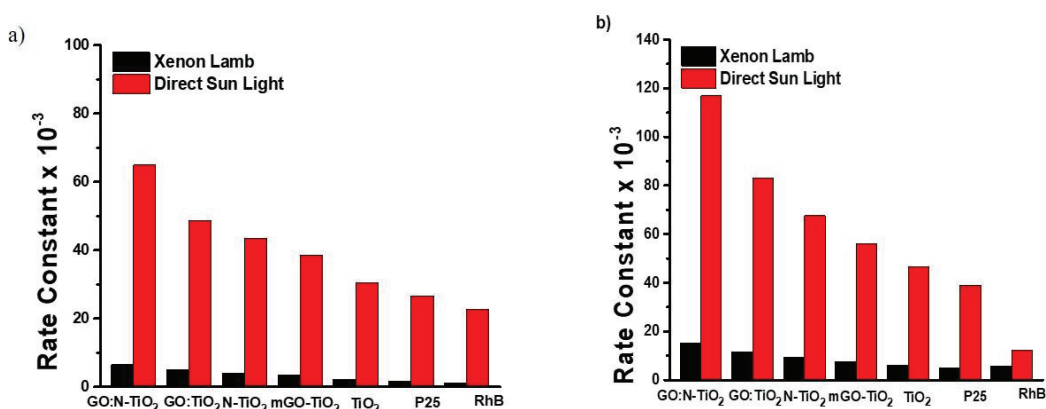

Figure 3. 14. Comparison of degradation rate constants of a) non-sensitized catalysts and b) PTE sensitized catalysts.

As shown in Figure 3. 14, there is a significant difference between the rate constants of photocatalytic studies performed under the Xe lamp and direct sunlight.

This is obviously due to the fact that the intensity of direct sunlight (800 ± 45 W / m^2) is much higher than the Xe lamp (190 ± 7 W/m2). Under the higher intensity of light irradiation, the enhancement was considerably higher because there were more photons per unit time and unit area for the photo-activation of catalyst surface, therefore the enhancement of the degradation rate with direct sun light can be attributed to the photocatalytic power which is stronger. The measurements showed that the intensity of the direct sunlight on the day of the experiments performed was 4 times higher than the intensity of the Xe lamp. However, the increase of degradation rate constants under direct sun light is much higher than 4 factors compared to the Xe lamp. This also indicated that different photocatalytic activities occur under different light sources. Cruz et al. reported that during the photocatalytic activity of TiO_2 under UV light, only hydroxyl radicals are formed in the medium. However, superoxide radicals and singlet oxygen are formed under visible light and lead to degradation more effectively and faster than the degradation under Xe lamp (Cruz et al. 2017). Therefore, the better photocatalytic activity in the study is based on the fact that the intensity is higher and the production of superoxide and singlet oxygen as well as hydroxyl radical.

CHAPTER 4

CONCLUSION

In this study, mGO-TiO$_2$ composite was synthesized using the low temperature hydrothermal method and catalyst films P25, TiO$_2$, N-TiO$_2$, mGO-TiO$_2$, GO-TiO$_2$ and GO:N-TiO$_2$ were fabricated by the doctor blade method. Characterization of the synthesized material was carried out using X-ray diffraction method, X-ray photoelectron spectroscopy, and BET analysis techniques and the results supported the composite formation of TiO$_2$ with GO / mGO.

The photocatalytic activity of the fabricated films was investigated in degradation of the RhB dye under direct sunlight and under Xe lamp. As a result of these studies, the photocatalytic activity order of the photocatalysts is as follows:
GO: N-TiO$_2$ > GO:TiO$_2$ > N-TiO$_2$ > mGO:TiO$_2$ > TiO$_2$ > P25.
The composite catalysts exhibited better photocatalytic activity than that of bare TiO$_2$ due to great electrical and optical properties of GO. The composite catalysts adsorbed more dye than other catalysts due to their adsorptive ability, which is due to having oxygen-containing functional groups (Rong et al. 2015). Thus, improvement of photocatalytic activity by GO -TiO$_2$ / N-TiO$_2$ composite formation is attributed to increase adsorptive ability and tminimize the aggregation of TiO$_2$ nanoparticles and recombination of e - h pairs.

In the study, GO:N-TiO$_2$ film showed the best photocatalytic performance, implying that the charge carriers were separated more effectively due to the cooperative effect of N doping and composite formation with GO in the study.

The lower performance of mGO:TiO$_2$ may also be attributed to the disappear of hydroxyl groups which are responsible in adsorption of dye molecules in the structure. The electrons from TiO$_2$ may be trapped and have negatively affected the formation of the superoxide radical which is also responsible in oxidation-reduction.

PTE dye sensitized TiO$_2$ films exhibited greater photocatalytic activity than non-sensitized TiO$_2$ films. Although the order of photocatalytic activity did not change, the photocatalytic rate constants significantly increased. It is attributed that PTE sensitizer extend the photoactivity of TiO$_2$ to the visible region corresponding to a bandgap of 2.5

eV and its well matched energy levels to TiO_2 and hence improve the electrical charge transport.

The degradation rate constants slightly decrease after second and third utilizations and therefore fabricated films have suitable reusability.

The PTE dye sensitization of TiO_2 composites has been proven to be one of the easiest and practical approaches for utilizing visible light as a result of photocatalytic activity studies under direct sun light.

REFERENCES

Adebowale, Kayode O., Bamidele I. Olu-Owolabi, and Emmanuel C. Chigbundu. 2014. "Removal of Safranin-O from Aqueous Solution by Adsorption onto Kaolinite Clay." *Journal of Encapsulation and Adsorption Sciences* 04 (03): 89–104. https://doi.org/10.4236/jeas.2014.43010.

Ahmed, Syed Nabeel, and Waseem Haider. 2018. "Heterogeneous Photocatalysis and Its Potential Applications in Water and Wastewater Treatment: A Review." *Nanotechnology* 29 (34). https://doi.org/10.1088/1361-6528/aac6ea.

Alazmi, Amira, Shahid Rasul, Shashikant P. Patole, and Pedro M.F.J. Costa. 2016. "Comparative Study of Synthesis and Reduction Methods for Graphene Oxide." *Polyhedron* 116: 153–61. https://doi.org/10.1016/j.poly.2016.04.044.

Ali, Imran. 2012. "New Generation Adsorbents for Water Treatment." *Chemical Reviews* 112 (10): 5073–91. https://doi.org/10.1021/cr300133d.

Benjwal, Poonam, Manish Kumar, Pankaj Chamoli, and Kamal K. Kar. 2015. "Enhanced Photocatalytic Degradation of Methylene Blue and Adsorption of Arsenic(Iii) by Reduced Graphene Oxide (RGO)-Metal Oxide (TiO2/Fe3O4) Based Nanocomposites." *RSC Advances* 5 (89): 73249–60. https://doi.org/10.1039/c5ra13689j.

Cao, Yuan Cheng, Zhongtian Fu, Wenjun Wei, Linling Zou, Tie Mi, Dan He, Chaolu Yan, et al. 2015. "Reduced Graphene Oxide Supported Titanium Dioxide Nanomaterials for the Photocatalysis with Long Cycling Life." *Applied Surface Science*. https://doi.org/10.1016/j.apsusc.2015.08.036.

Cayci, Gamze Belkis. 2016. "GO:N-TiO2 ve GO:TiO2 Sentezi Ve Rhodamine B Fotodegradasyonunda Fotokatalitik Aktivitesinin İncelenmesi." Ege Üniversitesi.

Chowdhury, Pankaj, Ghodsieh Malekshoar, and Ajay K. Ray. 2017. "Dye-Sensitized Photocatalytic Water Splitting and Sacrificial Hydrogen Generation: Current Status and Future Prospects." *Inorganics* 5 (2). https://doi.org/10.3390/inorganics5020034.

Cruz, Marta, Cristina Gomez, Carlos J. Duran-Valle, Luisa M. Pastrana-Martínez, Joaquim L. Faria, Adrián M.T. Silva, Marisol Faraldos, and Ana Bahamonde. 2017. "Bare TiO 2 and Graphene Oxide TiO 2 Photocatalysts on the Degradation of Selected Pesticides and Influence of the Water Matrix." *Applied Surface Science* 416: 1013–21. https://doi.org/10.1016/j.apsusc.2015.09.268.

Diker, Halide. 2017. "Organik Fotonik Sistemlerde Kullanilabilecek Grafen Oksit Sentezi Ve Karakterizasyonu." Ege Üniversitesi.

Diker, Halide, Hakan Bozkurt, and Canan Varlikli. 2020. "Dispersion Stability of Amine Modified Graphene Oxides and Their Utilization in Solution Processed Blue OLED." *Chemical Engineering Journal* 381 (June 2019): 122716. https://doi.org/10.1016/j.cej.2019.122716.

Diker, Halide, Canan Varlikli, Koray Mizrak, and Aykutlu Dana. 2011. "Characterizations and Photocatalytic Activity Comparisons of N-Doped Nc-TiO2 Depending on Synthetic Conditions and Structural Differences of Amine Sources." *Energy* 36 (2): 1243–54. https://doi.org/10.1016/j.energy.2010.11.020.

Diker, Halide, Canan Varlikli, and Elias Stathatos. 2014. "N-Doped Titania Powders Prepared by Different Nitrogen Sources and Their Application in Quasi-Solid State Dye-Sensitized Solar Cells." *International Journal of Energy Research* 38: 908–17. https://doi.org/10.1002/er3091.

Dong, Shuying, Jinglan Feng, Maohong Fan, Yunqing Pi, Limin Hu, Xiao Han, Menglin Liu, Jingyu Sun, and Jianhui Sun. 2015. "Recent Developments in Heterogeneous Photocatalytic Water Treatment Using Visible Light-Responsive Photocatalysts: A Review." *RSC Advances* 5 (19): 14610–30. https://doi.org/10.1039/c4ra13734e.

Drahansky, Martin, M.t Paridah, Amin Moradbak, A.Z Mohamed, Folahan abdulwahab taiwo Owolabi, Mustapha Asniza, and Shawkataly H.P Abdul Khalid. 2016. "We Are IntechOpen , the World ' s Leading Publisher of Open Access Books Built by Scientists , for Scientists TOP 1 %." *Intech* i (tourism): 13. https://doi.org/http://dx.doi.org/10.5772/57353.

Ersundu, Ali Erçin. 2017. "Investigation of Photocatalytic Activity of Sol-Gel Derived

Boron and/or Nitrogen Doped TiO2 Powder and Thin Films Under UV and Visible Light." *Afyon Kocatepe University Journal of Sciences and Engineering* 17 (1): 227–38. https://doi.org/10.5578/fmbd.53936.

Frank, Steven N., and Allen J. Bard. 1977. "Heterogeneous Photocatalytic Oxidation of Cyanide and Sulfite in Aqueous Solutions at Semiconductor Powders." *Journal of Physical Chemistry* 81 (15): 1484–88. https://doi.org/10.1021/j100530a011.

Fu, Changjing, Guogang Zhao, Haijun Zhang, and Shuang Li. 2013. "Evaluation and Characterization of Reduced Graphene Oxide Nanosheets as Anode Materials for Lithium-Ion Batteries." *International Journal of Electrochemical Science* 8 (5): 6269–80.

Fujima, A., Honda, K. 1972. "Electrochemical Photolysis of Water at a Semiconductor Electrode." *Nature* 238 (5358): 38–40. https://doi.org/10.1038/238038a0.

Fujishima, Akira, Xintong Zhang, and Donald A. Tryk. 2008. "TiO2 Photocatalysis and Related Surface Phenomena." *Surface Science Reports* 63 (12): 515–82. https://doi.org/10.1016/j.surfrep.2008.10.001.

Fulari, A. V., M. V. Ramana Reddy, S. T. Jadhav, G. S. Ghodake, Dae Young Kim, and G. M. Lohar. 2018. "TiO2/Reduced Graphene Oxide Composite Based Nano-Petals for Supercapacitor Application: Effect of Substrate." *Journal of Materials Science: Materials in Electronics* 29 (13): 10814–24. https://doi.org/10.1007/s10854-018-9146-5.

Gao, Yanyan, Xipeng Pu, Dafeng Zhang, Guqiao Ding, Xin Shao, and Jing Ma. 2012a. "Combustion Synthesis of Graphene Oxide-TiO 2 Hybrid Materials for Photodegradation of Methyl Orange." *Carbon* 50 (11): 4093–4101. https://doi.org/10.1016/j.carbon.2012.04.057.

———. 2012b. "Combustion Synthesis of Graphene Oxide-TiO 2 Hybrid Materials for Photodegradation of Methyl Orange." *Carbon*. https://doi.org/10.1016/j.carbon.2012.04.057.

Gaya, Umar Ibrahim, and Abdul Halim Abdullah. 2008. "Heterogeneous Photocatalytic Degradation of Organic Contaminants over Titanium Dioxide: A Review of

Fundamentals, Progress and Problems." *Journal of Photochemistry and Photobiology C: Photochemistry Reviews* 9 (1): 1–12. https://doi.org/10.1016/j.jphotochemrev.2007.12.003.

Georgakilas, Vasilios, Michal Otyepka, Athanasios B. Bourlinos, Vimlesh Chandra, Namdong Kim, K. Christian Kemp, Pavel Hobza, Radek Zboril, and Kwang S. Kim. 2012. "Functionalization of Graphene: Covalent and Non-Covalent Approaches, Derivatives and Applications." *Chemical Reviews* 112 (11): 6156–6214. https://doi.org/10.1021/cr3000412.

Georgakilas, Vasilios, Jitendra N. Tiwari, K. Christian Kemp, Jason A. Perman, Athanasios B. Bourlinos, Kwang S. Kim, and Radek Zboril. 2016. "Noncovalent Functionalization of Graphene and Graphene Oxide for Energy Materials, Biosensing, Catalytic, and Biomedical Applications." *Chemical Reviews* 116 (9): 5464–5519. https://doi.org/10.1021/acs.chemrev.5b00620.

Gerven, Tom Van, Guido Mul, Jacob Moulijn, and Andrzej Stankiewicz. 2007. "A Review of Intensification of Photocatalytic Processes." *Chemical Engineering and Processing: Process Intensification* 46 (9 SPEC. ISS.): 781–89. https://doi.org/10.1016/j.cep.2007.05.012.

Gu, Liuan, Jingyu Wang, Hao Cheng, Yizhi Zhao, Lifei Liu, and Xijiang Han. 2013. "One-Step Preparation of Graphene-Supported Anatase TiO2 with Exposed {001} Facets and Mechanism of Enhanced Photocatalytic Properties." *ACS Applied Materials and Interfaces* 5 (8): 3085–93. https://doi.org/10.1021/am303274t.

Guillard, Chantal, Eric Puzenat, Hinda Lachheb, Ammar Houas, and Jean Marie Herrmann. 2005. "Why Inorganic Salts Decrease the TiO2 Photocatalytic Efficiency." *International Journal of Photoenergy* 7 (1): 1–9. https://doi.org/10.1155/S1110662X05000012.

Hudaya, Tedi. 2008. "Synthesis, Characterisation and Activity of Nowel TiO2-Based Photocatalysts for Organic Pollutant Photodestruction under UV and Visible Light Irradation." *Sch. Chem. Sci.Eng*.

Hummers, William S., and Richard E. Offeman. 1958. "Preparation of Graphitic Oxide." *Journal of the American Chemical Society* 80 (6): 1339.

https://doi.org/10.1021/ja01539a017.

Hunger, Klaus. 2017. *Industrial Dyes Chemistry, Properties, Applications*. *IRYO - Japanese Journal of National Medical Services*. Vol. 71.

Ismail, Adel A., R. A. Geioushy, Houcine Bouzid, Saleh A. Al-Sayari, Ali Al-Hajry, and Detlef W. Bahnemann. 2013. "TiO2 Decoration of Graphene Layers for Highly Efficient Photocatalyst: Impact of Calcination at Different Gas Atmosphere on Photocatalytic Efficiency." *Applied Catalysis B: Environmental* 129: 62–70. https://doi.org/10.1016/j.apcatb.2012.09.024.

Jaihindh, Dhayanantha Prabu, Ching Cheng Chen, and Yen Pei Fu. 2018. "Reduced Graphene Oxide-Supported Ag-Loaded Fe-Doped TiO2 for the Degradation Mechanism of Methylene Blue and Its Electrochemical Properties." *RSC Advances* 8 (12): 6488–6501. https://doi.org/10.1039/c7ra13418e.

Jing, Jieying, Yang Zhang, Wenying Li, and William W. Yu. 2014. "Visible Light Driven Photodegradation of Quinoline over TiO 2 /Graphene Oxide Nanocomposites." *Journal of Catalysis* 316: 174–81. https://doi.org/10.1016/j.jcat.2014.05.009.

Karapire, C., M. Kus, G. Turkmen, C.C. C. Trevithick-Sutton, C.S. S. Foote, and S. Icli. 2005. "Photooxidation Studies with Perylenediimides in Solution, PVC and Sol–Gel Thin Films under Concentrated Sun Light." *Solar Energy* 78 (1): 5–17. https://doi.org/10.1016/j.solener.2004.07.003.

Karapire, Canan, Ceylan Zafer, and Sıddık İçli. 2004. "Studies on Photophysical and Electrochemical Properties of Synthesized Hydroxy Perylenediimides in Nanostructured Titania Thin Films." *Synthetic Metals* 145 (1): 51–60. https://doi.org/10.1016/j.synthmet.2004.04.016.

Khalid, N. R., E. Ahmed, Zhanglian Hong, Yuewei Zhang, and M. Ahmad. 2012. "Nitrogen Doped TiO 2 Nanoparticles Decorated on Graphene Sheets for Photocatalysis Applications." *Current Applied Physics*. https://doi.org/10.1016/j.cap.2012.04.019.

Krishnamoorthy, Karthikeyan, Murugan Veerapandian, Kyusik Yun, and S. J. Kim.

2013. "The Chemical and Structural Analysis of Graphene Oxide with Different Degrees of Oxidation." *Carbon* 53: 38–49. https://doi.org/10.1016/j.carbon.2012.10.013.

Kuila, Tapas, Saswata Bose, Ananta Kumar Mishra, Partha Khanra, Nam Hoon Kim, and Joong Hee Lee. 2012. "Chemical Functionalization of Graphene and Its Applications." *Progress in Materials Science*. https://doi.org/10.1016/j.pmatsci.2012.03.002.

Kus, Mahmut, Özgül Hakli, Ceylan Zafer, Canan Varlikli, Serafettin Demic, Serdar Özçelik, and Siddik Icli. 2008. "Optical and Electrochemical Properties of Polyether Derivatives of Perylenediimides Adsorbed on Nanocrystalline Metal Oxide Films." *Organic Electronics: Physics, Materials, Applications* 9 (5): 757–66. https://doi.org/10.1016/j.orgel.2008.05.009.

Lerf, Anton, Heyong He, Michael Forster, and Jacek Klinowski. 1998. "Structure of Graphite Oxide Revisited." *Journal of Physical Chemistry B* 102 (23): 4477–82. https://doi.org/10.1021/jp9731821.

Li, Wenjuan, Xiu Zhi Tang, Hao Bin Zhang, Zhi Guo Jiang, Zhong Zhen Yu, Xu Sheng Du, and Yiu Wing Mai. 2011. "Simultaneous Surface Functionalization and Reduction of Graphene Oxide with Octadecylamine for Electrically Conductive Polystyrene Composites." *Carbon*. https://doi.org/10.1016/j.carbon.2011.06.077.

Li, Wenqiang, Xiang Liu, and Hexing Li. 2015. "Hydrothermal Synthesis of Graphene/Fe3+-Doped TiO2 Nanowire Composites with Highly Enhanced Photocatalytic Activity under Visible Light Irradiation." *Journal of Materials Chemistry A* 3 (29): 15214–24. https://doi.org/10.1039/c5ta00763a.

Li, Youji, Feitai Chen, Rongan He, Yingchun Wang, and Ningmei Tang. 2019. *Semiconductor Photocatalysis for Water Purification*. *Nanoscale Materials in Water Purification*. Elsevier Inc. https://doi.org/10.1016/b978-0-12-813926-4.00030-6.

Liu, Lei, Hongwei Bai, Jincheng Liu, and Darren D. Sun. 2013. "Multifunctional Graphene Oxide-TiO2-Ag Nanocomposites for High Performance Water Disinfection and Decontamination under Solar Irradiation." *Journal of Hazardous*

Materials 261: 214–23. https://doi.org/10.1016/j.jhazmat.2013.07.034.

Lonkar, Sunil P., Yogesh S. Deshmukh, and Ahmed A. Abdala. 2015. "Recent Advances in Chemical Modifications of Graphene." *Nano Research* 8 (4): 1039–74. https://doi.org/10.1007/s12274-014-0622-9.

Lu, Y. H., W. Chen, Y. P. Feng, and P. M. He. 2009. "Tuning the Electronic Structure of Graphene by an Organic Molecule." *Journal of Physical Chemistry B* 113 (1): 2–5. https://doi.org/10.1021/jp806905e.

Mahmoodi, Niyaz Mohammad, Mokhtar Arami, Nargess Yousefi Limaee, and Nooshin Salman Tabrizi. 2005. "Decolorization and Aromatic Ring Degradation Kinetics of Direct Red 80 by UV Oxidation in the Presence of Hydrogen Peroxide Utilizing TiO2 as a Photocatalyst." *Chemical Engineering Journal* 112 (1–3): 191–96. https://doi.org/10.1016/j.cej.2005.07.008.

Marcano, Daniela C., Dmitry V. Kosynkin, Jacob M. Berlin, Alexander Sinitskii, Zhengzong Sun, Alexander Slesarev, Lawrence B. Alemany, Wei Lu, and James M. Tour. 2010. "Improved Synthesis of Graphene Oxide." *ACS Nano* 4 (8): 4806–14. https://doi.org/10.1021/nn1006368.

Maruthamani, D., D. Divakar, and M. Kumaravel. 2015. "Enhanced Photocatalytic Activity of TiO2 by Reduced Graphene Oxide in Mineralization of Rhodamine B Dye." *Journal of Industrial and Engineering Chemistry* 30: 33–43. https://doi.org/10.1016/j.jiec.2015.04.026.

Mattos, Jonatas Batista, Kaique Brito Silva, Roberto José Silva, Thiara Helena Mota Almeida, Hogana Sibilla Soares Póvoas, Paulo Vagner Ribeiro Silva, Ingrid Matos de Araújo Góes, and Irlanda Silva Matos. 2019. "Natural Factors or Environmental Neglect? Understanding the Dilemma of a Water Crisis in a Scenario of Water Plenty." *Land Use Policy*. https://doi.org/10.1016/j.landusepol.2018.12.027.

Munjal, Guncha, Amita Choudhary, Garima Dwivedi, and Ashok N Bhaskarwar. 2017. "Heterogeneous Photocatalysis in Wastewater Treatment-A Review" 04 (13): 903–7.

Nguyen-Phan, Thuy Duong, Viet Hung Pham, Eun Woo Shin, Hai Dinh Pham,

Sunwook Kim, Jin Suk Chung, Eui Jung Kim, and Seung Hyun Hur. 2011. "The Role of Graphene Oxide Content on the Adsorption-Enhanced Photocatalysis of Titanium Dioxide/Graphene Oxide Composites." *Chemical Engineering Journal* 170 (1): 226–32. https://doi.org/10.1016/j.cej.2011.03.060.

Nosaka, Yoshio, and Atsuko Nosaka. 2016. "Understanding Hydroxyl Radical (•OH) Generation Processes in Photocatalysis." *ACS Energy Letters* 1 (2): 356–59. https://doi.org/10.1021/acsenergylett.6b00174.

Novoselov, K. S., A. K. Geim, S V Morozov, Da Jiang, Yanshui Zhang, S. V. Dubonos, Irina V Grigorieva, and A. A. Firsov. 2004. "Electric Field Effect in Atomically Thin Carbon Films Supplementary." *Science* 5 (1): 1–12. https://doi.org/10.1126/science.aab1343.

Parent, Yves, Daniel Blake, Kim Magrini-Bair, Carol Lyons, Craig Turchi, Andy Watt, Edward Wolfrum, and Michael Prairie. 1996. "Solar Photocatalytic Processes for the Purification of Water: State of Development and Barriers to Commercialization." *Solar Energy*. https://doi.org/10.1016/0038-092X(96)81767-1.

Park, Sungjin, and Rodney S. Ruoff. 2009. "Chemical Methods for the Production of Graphenes." *Nature Nanotechnology* 4 (4): 217–24. https://doi.org/10.1038/nnano.2009.58.

Pastrana-Martínez, Luisa M., Sergio Morales-Torres, Vlassis Likodimos, José L. Figueiredo, Joaquim L. Faria, Polycarpos Falaras, and Adrián M.T. Silva. 2012. "Advanced Nanostructured Photocatalysts Based on Reduced Graphene Oxide-TiO2 Composites for Degradation of Diphenhydramine Pharmaceutical and Methyl Orange Dye." *Applied Catalysis B: Environmental*. https://doi.org/10.1016/j.apcatb.2012.04.045.

Patel, Jankhan, and Amirkianoosh Kiani. 2019. "Effects of Reduced Graphene Oxide (RGO) at Different Concentrations on Tribological Properties of Liquid Base Lubricants." *Lubricants* 7 (2). https://doi.org/10.3390/lubricants7020011.

Pu, Xipeng, Dafeng Zhang, Yanyan Gao, Xin Shao, Guqiao Ding, Songsong Li, and Shuping Zhao. 2013. "One-Pot Microwave-Assisted Combustion Synthesis of

Graphene Oxide-TiO 2 Hybrids for Photodegradation of Methyl Orange." *Journal of Alloys and Compounds* 551: 382–88. https://doi.org/10.1016/j.jallcom.2012.11.028.

Purkait, M. K., S. S. Vijay, S. DasGupta, and S. De. 2004. "Separation of Congo Red by Surfactant Mediated Cloud Point Extraction." *Dyes and Pigments* 63 (2): 151–59. https://doi.org/10.1016/j.dyepig.2004.01.010.

Ramesha, G. K., A. Vijaya Kumara, H. B. Muralidhara, and S. Sampath. 2011. "Graphene and Graphene Oxide as Effective Adsorbents toward Anionic and Cationic Dyes." *Journal of Colloid and Interface Science* 361 (1): 270–77. https://doi.org/10.1016/j.jcis.2011.05.050.

Rauf, M. A., M. A. Meetani, and S. Hisaindee. 2011. "An Overview on the Photocatalytic Degradation of Azo Dyes in the Presence of TiO2 Doped with Selective Transition Metals." *Desalination* 276 (1–3): 13–27. https://doi.org/10.1016/j.desal.2011.03.071.

Reynel-Avila, H. E., D. I. Mendoza-Castillo, and A. Bonilla-Petriciolet. 2016. "Relevance of Anionic Dye Properties on Water Decolorization Performance Using Bone Char: Adsorption Kinetics, Isotherms and Breakthrough Curves." *Journal of Molecular Liquids* 219: 425–34. https://doi.org/10.1016/j.molliq.2016.03.051.

Robinson, Tim, Geoff McMullan, Roger Marchant, and Poonam Nigam. 2001. "Remediation of Dyes in Textile Effluent: A Critical Review on Current Treatment Technologies with a Proposed Alternative." *Bioresource Technology* 77 (3): 247–55. https://doi.org/10.1016/S0960-8524(00)00080-8.

Rong, Xinshan, Fengxian Qiu, Chen Zhang, Liang Fu, Yuanyuan Wang, and Dongya Yang. 2015. "Preparation, Characterization and Photocatalytic Application of TiO2-Graphene Photocatalyst under Visible Light Irradiation." *Ceramics International* 41 (2): 2502–11. https://doi.org/10.1016/j.ceramint.2014.10.072.

Salavagione, Horacio J., Marián A. Gómez, and Gerardo Martínez. 2009. "Polymeric Modification of Graphene through Esterification of Graphite Oxide and Poly(Vinyl Alcohol)." *Macromolecules* 42 (17): 6331–34.

https://doi.org/10.1021/ma900845w.

Shang, Jing, Fengwei Zhao, Tong Zhu, and Jia Li. 2011. "Photocatalytic Degradation of Rhodamine B by Dye-Sensitized TiO2 under Visible-Light Irradiation." *Science China Chemistry* 54 (1): 167–72. https://doi.org/10.1007/s11426-010-4168-8.

Shanmugharaj, A. M., J. H. Yoon, W. J. Yang, and Sung Hun Ryu. 2013. "Synthesis, Characterization, and Surface Wettability Properties of Amine Functionalized Graphene Oxide Films with Varying Amine Chain Lengths." *Journal of Colloid and Interface Science* 401: 148–54. https://doi.org/10.1016/j.jcis.2013.02.054.

Shao, Gao Song, Xue Jun Zhang, and Zhong Yong Yuan. 2008. "Preparation and Photocatalytic Activity of Hierarchically Mesoporous-Macroporous TiO2-XNx." *Applied Catalysis B: Environmental*. https://doi.org/10.1016/j.apcatb.2008.01.026.

Sher Shah, Md Selim Arif, A. Reum Park, Kan Zhang, Jong Hyeok Park, and Pil J. Yoo. 2012. "Green Synthesis of Biphasic TiO 2-Reduced Graphene Oxide Nanocomposites with Highly Enhanced Photocatalytic Activity." *ACS Applied Materials and Interfaces* 4 (8): 3893–3901. https://doi.org/10.1021/am301287m.

Slokar, Y. M., and A. Majcen Le Marechal. 1998. "Methods of Decoloration of Textile Wastewaters." *Dyes and Pigments* 37 (4): 335–56. https://doi.org/10.1016/S0143-7208(97)00075-2.

Smalley, Richart E. 2005. "Future Global Energy Prosperity: The Terawatt Challange." *MRS Bull.* 30 (May): 412–17. https://doi.org/10.1557/mrs2005.124.

Sobczyński, A., and A. Dobosz. 2001. "Water Purification by Photocatalysis on Semiconductors." *Polish Journal of Environmental Studies* 10 (4): 195–205.

Sohail, Muhammad, Haoliang Xue, Qingze Jiao, Hansheng Li, Khakemin Khan, Shanshan Wang, and Yun Zhao. 2017. "Synthesis of Well-Dispersed TiO2@reduced Graphene Oxide (RGO) Nanocomposites and Their Photocatalytic Properties." *Materials Research Bulletin* 90: 125–30. https://doi.org/10.1016/j.materresbull.2017.02.025.

Szczepanik, Beata. 2017. "Photocatalytic Degradation of Organic Contaminants over

Clay-TiO2 Nanocomposites: A Review." *Applied Clay Science* 141: 227–39. https://doi.org/10.1016/j.clay.2017.02.029.

Tan, Lling Lling, Wee Jun Ong, Siang Piao Chai, Boon Tong Goh, and Abdul Rahman Mohamed. 2015. "Visible-Light-Active Oxygen-Rich TiO<inf>2</Inf> Decorated 2D Graphene Oxide with Enhanced Photocatalytic Activity toward Carbon Dioxide Reduction." *Applied Catalysis B: Environmental*. https://doi.org/10.1016/j.apcatb.2015.05.024.

Taşli, Pınar Tunay, Çiğdem Karabacak Atay, Tayfun Demirtürk, and Tahir Tilki. 2019. "Experimental and Computational Studies of Newly Synthesized Azo Dyes Based Materials." *Journal of Molecular Structure*. https://doi.org/10.1016/j.molstruc.2019.127098.

Terrones, Mauricio, Andrés R. Botello-Méndez, Jessica Campos-Delgado, Florentino López-Urías, Yadira I. Vega-Cantú, Fernando J. Rodríguez-Macías, Ana Laura Elías, et al. 2010. "Graphene and Graphite Nanoribbons: Morphology, Properties, Synthesis, Defects and Applications." *Nano Today* 5 (4): 351–72. https://doi.org/10.1016/j.nantod.2010.06.010.

Vallejo, William, Angie Rueda, Carlos Díaz-Uribe, Carlos Grande, and Patricia Quintana. 2019. "Photocatalytic Activity of Graphene Oxide-TiO 2 Thin Films Sensitized by Natural Dyes Extracted from Bactris Guineensis." *Royal Society Open Science* 6 (3). https://doi.org/10.1098/rsos.181824.

Varlikli and Diker in Aliofkhazraei, Mahmood. 2014. *Handbokk of Functional Nanomaterials Volume 3*.

Wan, Junmin, Meng Wei, Zhiwen Hu, Zhiqin Peng, Bing Wang, Daoyan Feng, and Yuewei Shen. 2016. "Ternary Composites of TiO2 Nanotubes with Reduced Graphene Oxide (RGO) and Meso-Tetra (4-Carboxyphenyl) Porphyrin for Enhanced Visible Light Photocatalysis." *International Journal of Hydrogen Energy* 41 (33): 14692–703. https://doi.org/10.1016/j.ijhydene.2016.07.053.

Wang, Dongting, Xin Li, Jianfeng Chen, and Xia Tao. 2012. "Enhanced Photoelectrocatalytic Activity of Reduced Graphene Oxide/TiO 2 Composite Films for Dye Degradation." *Chemical Engineering Journal*.

https://doi.org/10.1016/j.cej.2012.04.062.

Wang, Feng, and Kan Zhang. 2011a. "Reduced Graphene Oxide-TiO2 Nanocomposite with High Photocatalystic Activity for the Degradation of Rhodamine B." *Journal of Molecular Catalysis A: Chemical*. https://doi.org/10.1016/j.molcata.2011.05.026.

———. 2011b. "Reduced Graphene Oxide-TiO2 Nanocomposite with High Photocatalystic Activity for the Degradation of Rhodamine B." *Journal of Molecular Catalysis A: Chemical* 345 (1–2): 101–7. https://doi.org/10.1016/j.molcata.2011.05.026.

Wang, Jie, Tao Deng, Dawei Deng, Rong Zhang, Yueqing Gu, and Xiaoming Zha. 2016. "Quaternary Alloy Quantum Dots with Widely Tunable Emission-a Versatile System to Fabricate Dual-Emission Nanocomposites for Bio-Imaging." *RSC Advances* 6 (59): 53760–67. https://doi.org/10.1039/c6ra07407c.

Wang, Shuai, Perq Jon Chia, Lay Lay Chua, Li Hong Zhao, Rui Qi Png, Sankaran Sivaramakrishnan, Mi Zhou, et al. 2008. "Band-like Transport in Surface-Functionalized Highly Solution-Processable Graphene Nanosheets." *Advanced Materials* 20 (18): 3440–46. https://doi.org/10.1002/adma.200800279.

Wang, Xiuying, Jing Wang, Xiaoli Dong, Feng Zhang, Linge Ma, Xu Fei, Xiufang Zhang, and Hongchao Ma. 2016. "Synthesis and Catalytic Performance of Hierarchical TiO2 Hollow Sphere/Reduced Graphene Oxide Hybrid Nanostructures." *Journal of Alloys and Compounds*. https://doi.org/10.1016/j.jallcom.2015.09.241.

Wasylenko, Derek J., Ryan D. Palmer, Eduardo Schott, and Curtis P. Berlinguette. 2012. "Interrogation of Electrocatalytic Water Oxidation Mediated by a Cobalt Complex." *Chemical Communications* 48 (15): 2107–9. https://doi.org/10.1039/c2cc16674g.

Wei, Meng, Junmin Wan, Zhiwen Hu, Zhiqin Peng, and Bing Wang. 2016. "Enhanced Photocatalytic Degradation Activity over TiO 2 Nanotubes Co-Sensitized by Reduced Graphene Oxide and Copper(II) Meso-Tetra(4-Carboxyphenyl)Porphyrin." *Applied Surface Science* 377: 149–58.

https://doi.org/10.1016/j.apsusc.2016.03.120.

Xiang, Quanjun, Jiaguo Yu, and Mietek Jaroniec. 2012. "Graphene-Based Semiconductor Photocatalysts." *Chemical Society Reviews* 41 (2): 782–96. https://doi.org/10.1039/c1cs15172j.

Xiao, Lin, Li Youji, Chen Feitai, Xu Peng, and Li Ming. 2017. "Facile Synthesis of Mesoporous Titanium Dioxide Doped by Ag-Coated Graphene with Enhanced Visible-Light Photocatalytic Performance for Methylene Blue Degradation." *RSC Advances* 7 (41): 25314–24. https://doi.org/10.1039/c7ra02198d.

Yang, Dongxing, Aruna Velamakanni, Gülay Bozoklu, Sungjin Park, Meryl Stoller, Richard D. Piner, Sasha Stankovich, et al. 2009. "Chemical Analysis of Graphene Oxide Films after Heat and Chemical Treatments by X-Ray Photoelectron and Micro-Raman Spectroscopy." *Carbon*. https://doi.org/10.1016/j.carbon.2008.09.045.

Yang, Qiang, Xuejun Pan, Fang Huang, and Kecheng Li. 2010. "Fabrication of High-Concentration and Stable Aqueous Suspensions of Graphene Nanosheets by Noncovalent Functionalization with Lignin and Cellulose Derivatives." *Journal of Physical Chemistry C* 114 (9): 3811–16. https://doi.org/10.1021/jp910232x.

Yin, Xiong, Hailong Zhang, Peng Xu, Jing Han, Jianye Li, and Meng He. 2013. "Simultaneous N-Doping of Reduced Graphene Oxide and TiO2 in the Composite for Visible Light Photodegradation of Methylene Blue with Enhanced Performance." *RSC Advances* 3 (40): 18474–81. https://doi.org/10.1039/c3ra43403f.

Yoo, Dae Hwang, Tran Viet Cuong, Viet Hung Pham, Jin Suk Chung, Nguyen Tri Khoa, Eui Jung Kim, and Sung Hong Hahn. 2011. "Enhanced Photocatalytic Activity of Graphene Oxide Decorated on TiO 2 Films under UV and Visible Irradiation." *Current Applied Physics* 11 (3): 805–8. https://doi.org/10.1016/j.cap.2010.11.077.

Youssef, Zahraa, Ludovic Colombeau, Nurlykyz Yesmurzayeva, Francis Baros, Régis Vanderesse, Tayssir Hamieh, Joumana Toufaily, Céline Frochot, and Thibault Roques-Carmes. 2018. "Dye-Sensitized Nanoparticles for Heterogeneous

Photocatalysis: Cases Studies with TiO2, ZnO, Fullerene and Graphene for Water Purification." *Dyes and Pigments* 159 (May): 49–71. https://doi.org/10.1016/j.dyepig.2018.06.002.

Yu, Fei, Xueting Bai, Changfu Yang, Lijie Xu, and Jie Ma. 2019. "Reduced Graphene Oxide–P25 Nanocomposites as Efficient Photocatalysts for Degradation of Bisphenol A in Water." *Catalysts* 9 (7): 607. https://doi.org/10.3390/catal9070607.

Yuan, Rusheng, Rongbo Guan, Wenzhong Shen, and Jingtang Zheng. 2005. "Photocatalytic Degradation of Methylene Blue by a Combination of TiO 2 and Activated Carbon Fibers." *Journal of Colloid and Interface Science* 282 (1): 87–91. https://doi.org/10.1016/j.jcis.2004.08.143.

Zainuddin, M. F., N. H. Nik Raikhan, N. H. Othman, and W. F.H. Abdullah. 2018. "Synthesis of Reduced Graphene Oxide (RGO) Using Different Treatments of Graphene Oxide (GO)." *IOP Conference Series: Materials Science and Engineering* 358 (1): 0–6. https://doi.org/10.1088/1757-899X/358/1/012046.

Zhang, Yupeng, and Chunxu Pan. 2011. "TiO2/Graphene Composite from Thermal Reaction of Graphene Oxide and Its Photocatalytic Activity in Visible Light." *Journal of Materials Science* 46 (8): 2622–26. https://doi.org/10.1007/s10853-010-5116-x.

Zhao, Yanyan, Ke R. Yang, Zechao Wang, Xingxu Yan, Sufeng Cao, Yifan Ye, Qi Dong, et al. 2018. "Stable Iridium Dinuclear Heterogeneous Catalysts Supported on Metal-Oxide Substrate for Solar Water Oxidation." *Proceedings of the National Academy of Sciences of the United States of America* 115 (12): 2902–7. https://doi.org/10.1073/pnas.1722137115.
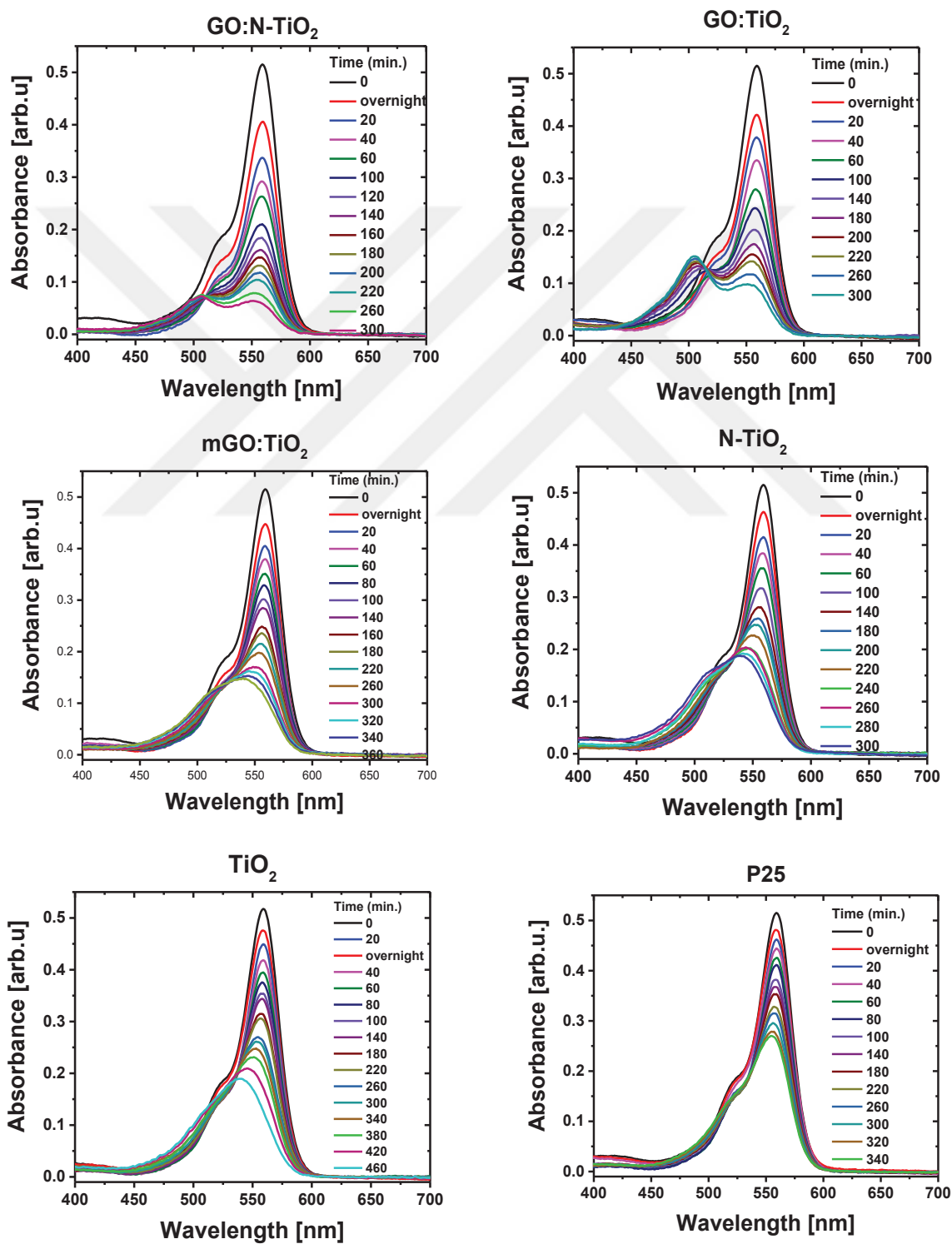
APPENDIX A

Degredation Profile of RhB under Xe Lamp Irradiation and Direct Sun Light without Catalyst Conditions
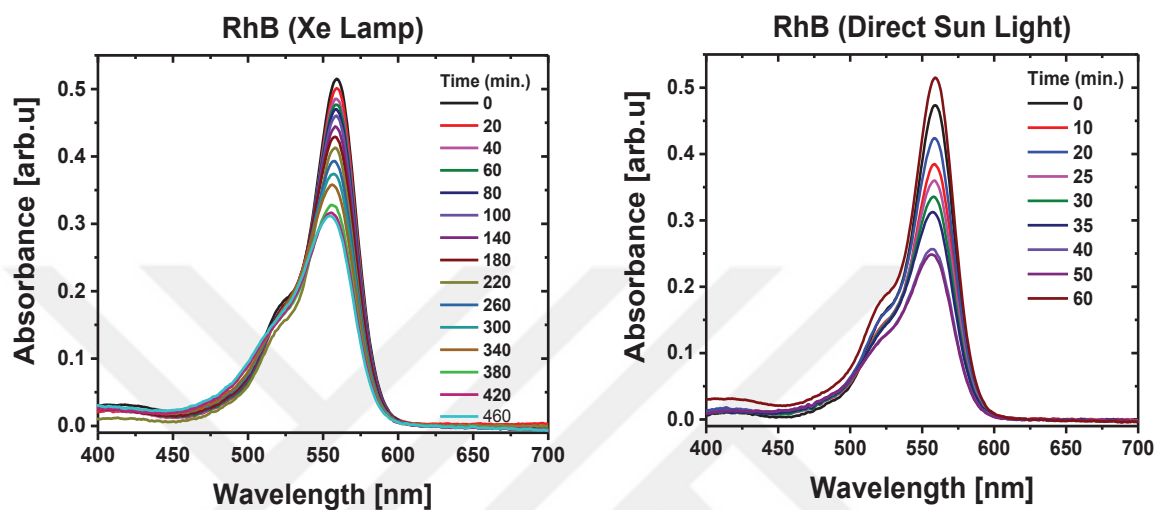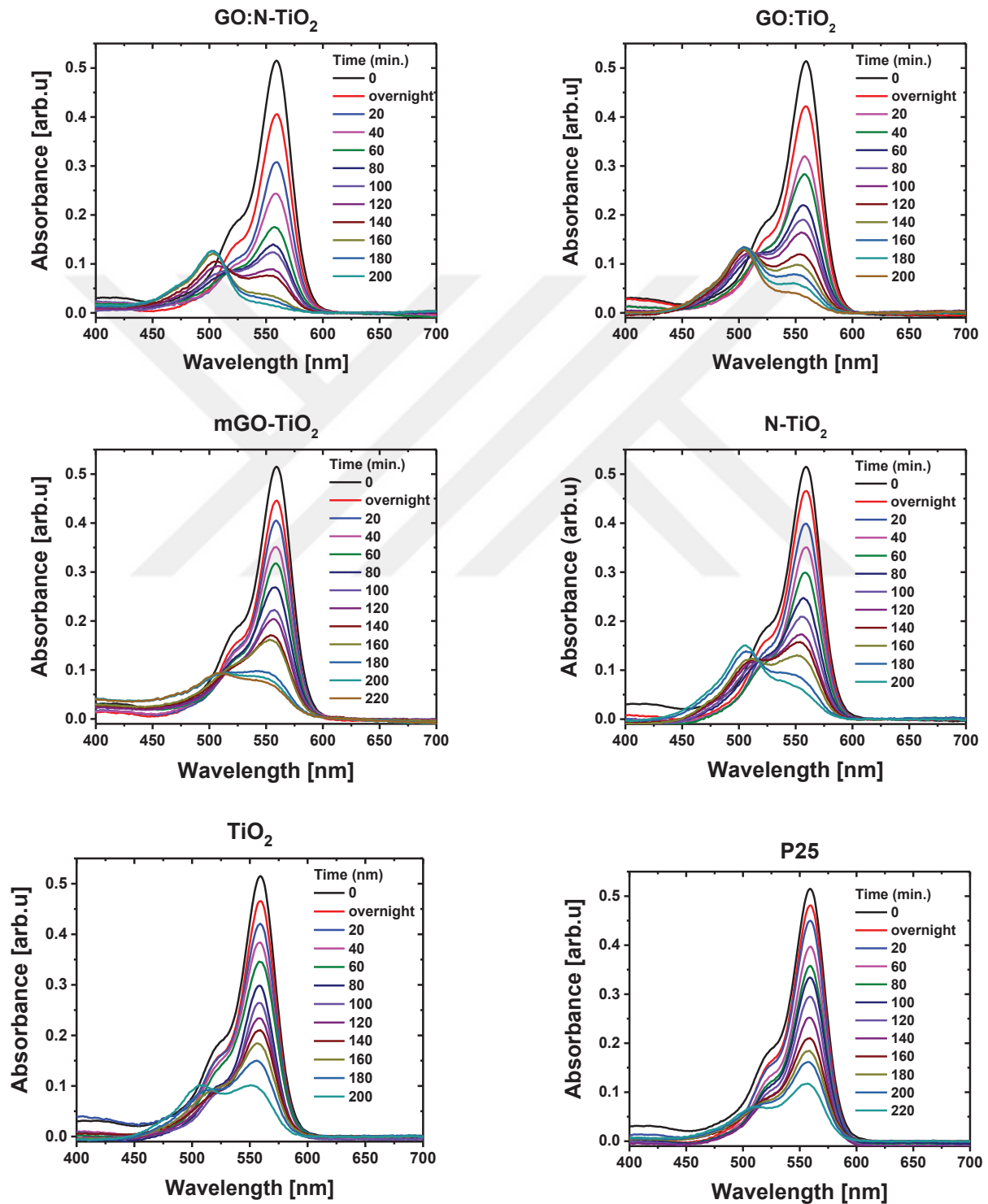
APPENDIX B

Degredation Profile of RhB under Xe Lamp Irradiation in Presence of Non-Sensitized Films (1st Cycle)
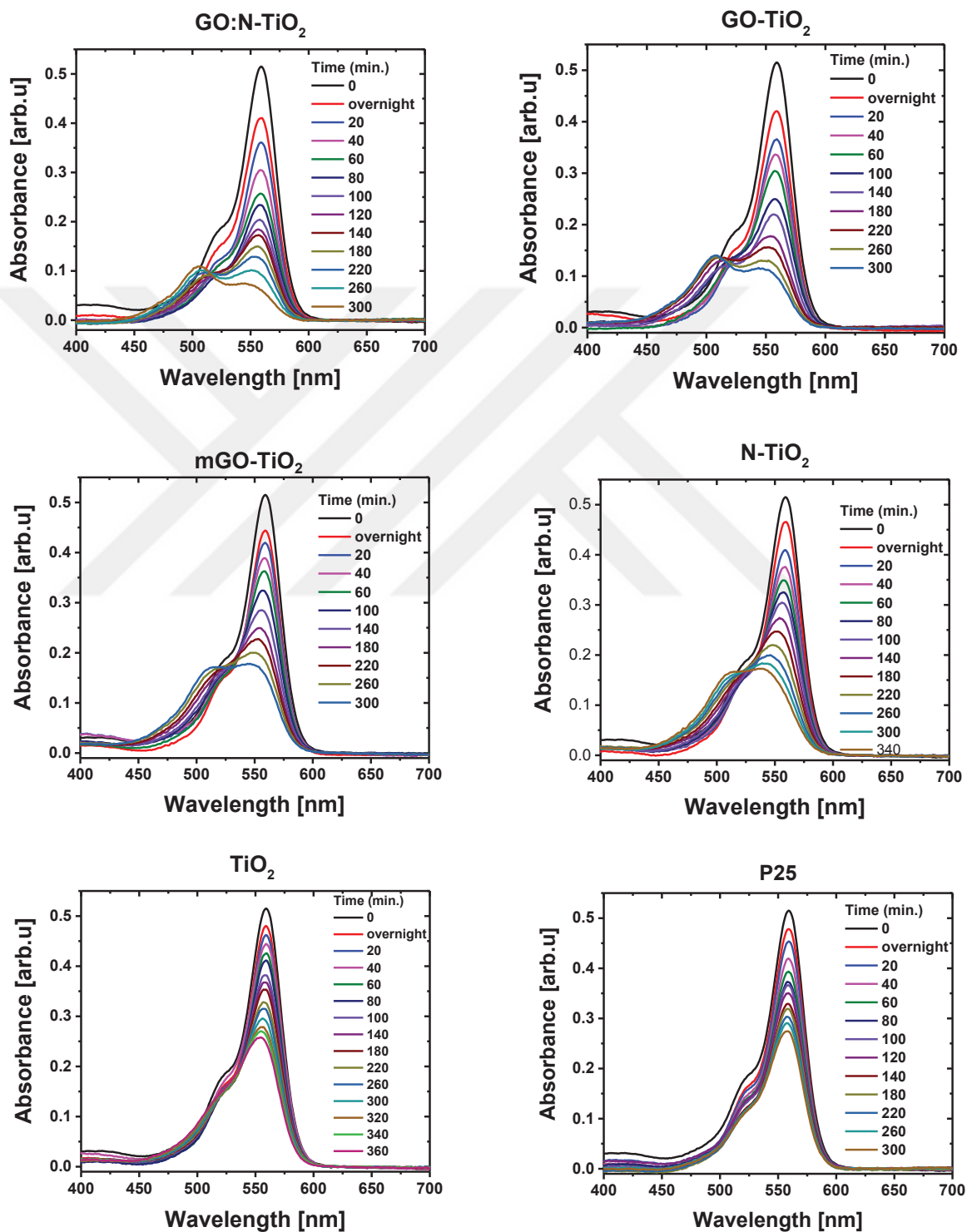
APPENDIX C

Degredation Profile of RhB under Xe Lamp Irradiation in Presence of PTE-Dye-Sensitized Films (1st Cycle)
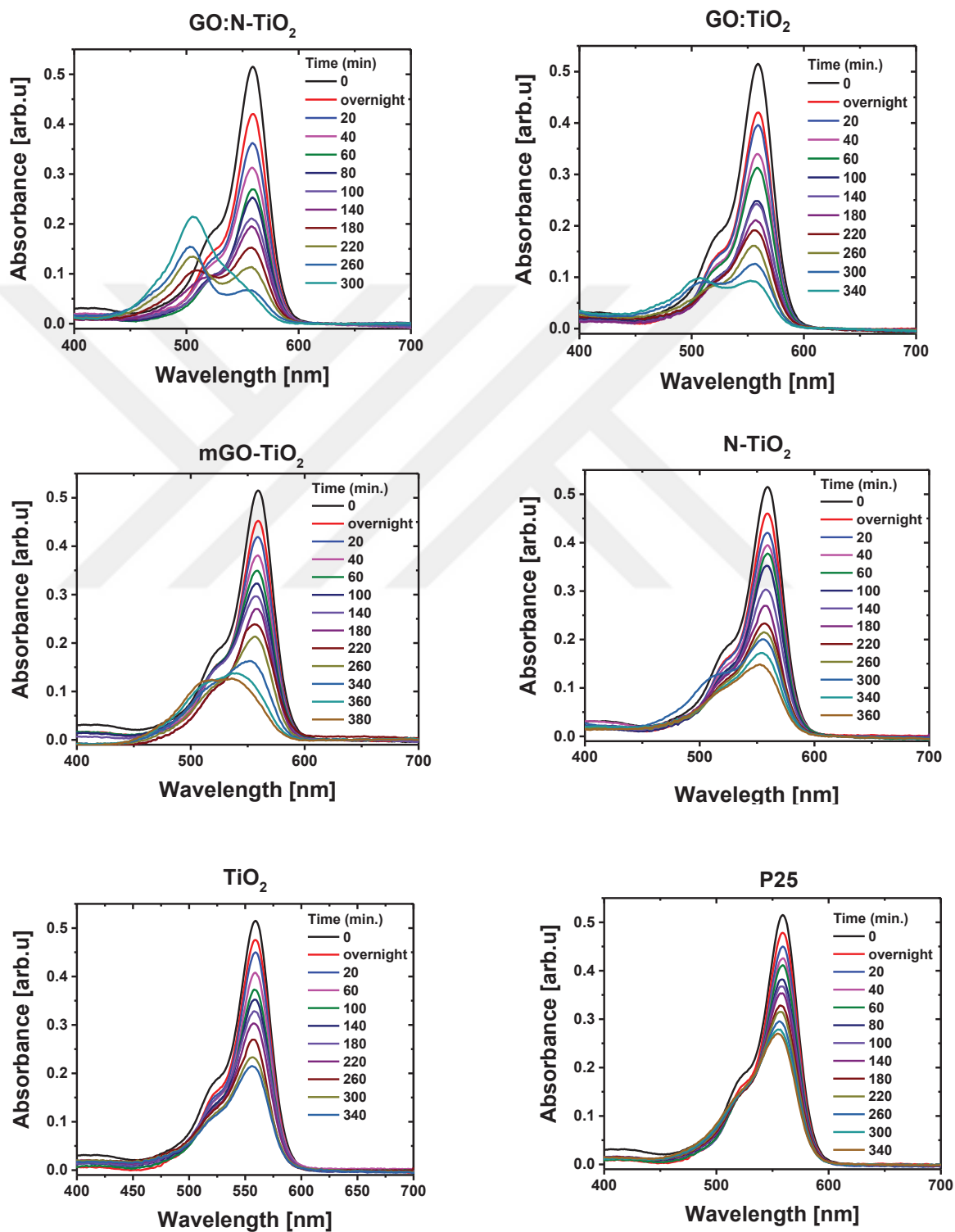
APPENDIX D

Degredation Profile of RhB under Xe Lamp Irradiation in Presence of Non-Sensitized Films (2nd Cycle)
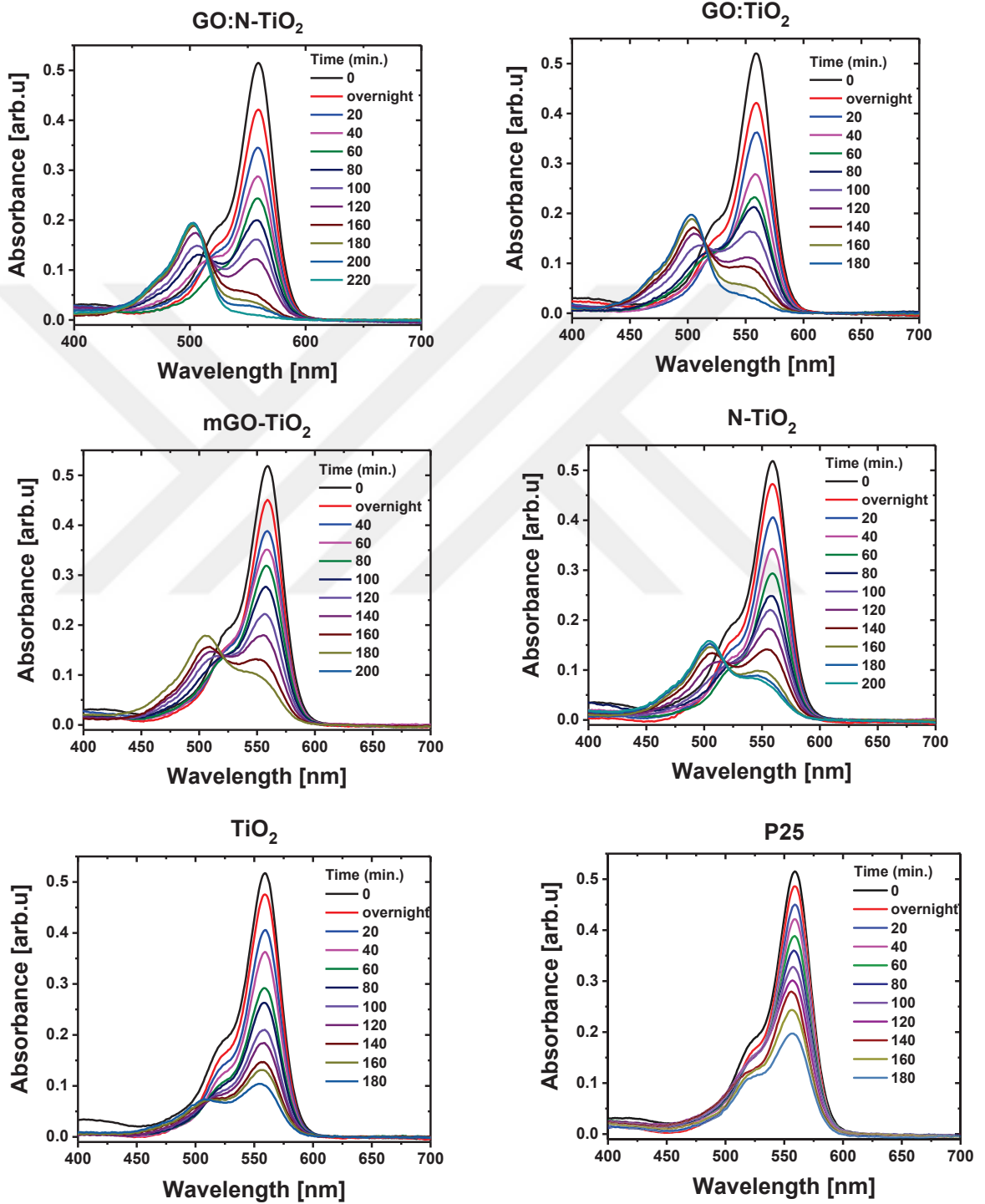
Degredation Profile of RhB under Xe Lamp Irradiation in Presence of Non-Sensitized Films (3rd Cycle)

APPENDIX F

Degredation Profile of RhB under Xe Lamp Irradiation in Presence of PTE-Dye-Sensitized Films (2nd Cycle)
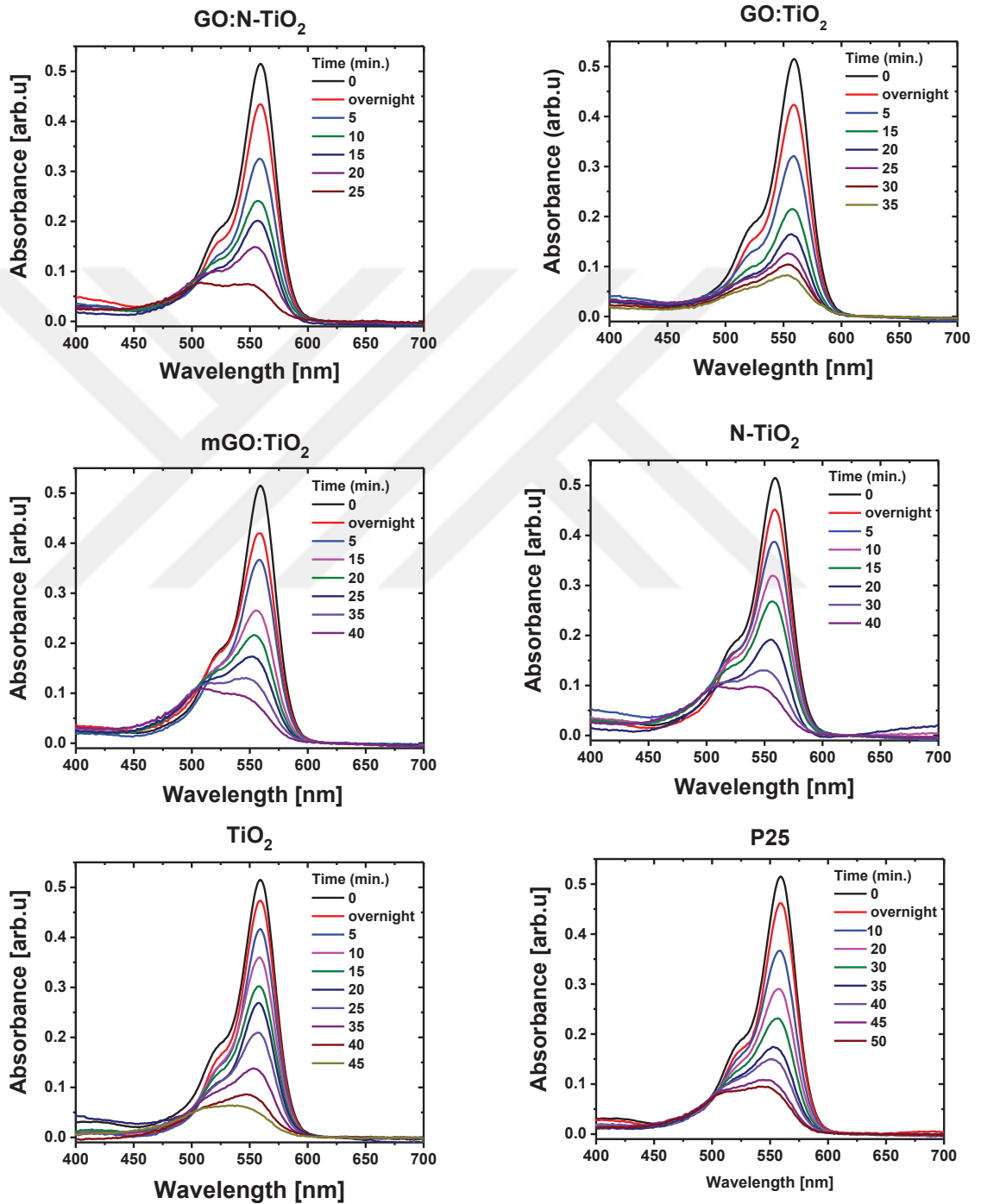

GO:N-TiO$_2$

GO:TiO$_2$

mGO-TiO$_2$

N-TiO$_2$

TiO$_2$

P25

APPENDIX G

Degredation Profile of RhB under Xe Lamp Irradiation in Presence of PTE-Dye-Sensitized Films (3rd Cycle)
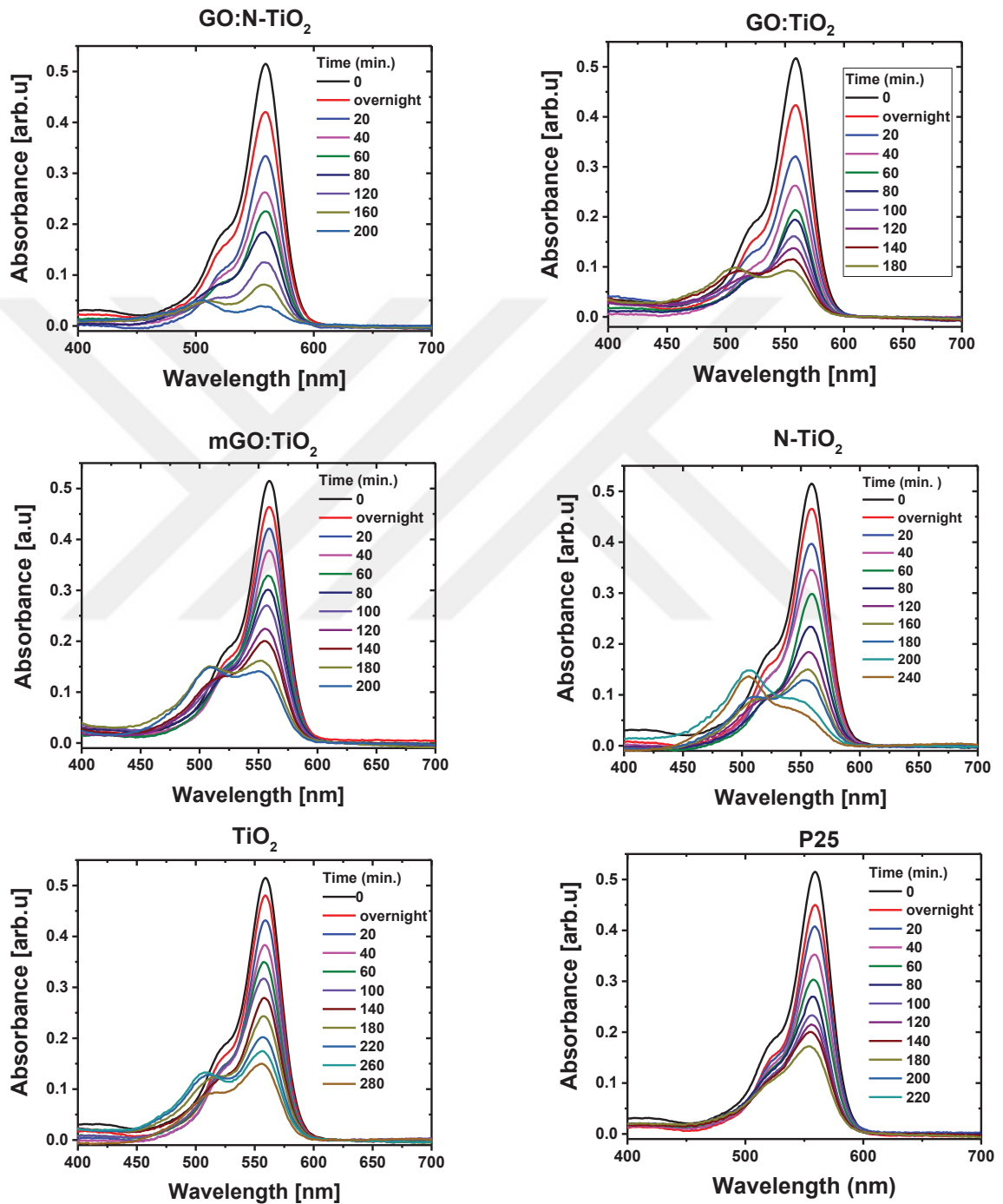
Degredation Profile of RhB under Direct Sun Light in Presence of Non-Sensitized Films

APPENDIX I

Degredation Profile of RhB under Direct Sun Light in Presence of PTE Dye-Sensitized Films